

NUCLEAR STRUCTURE -- EXPERIMENT

STUDY OF ( $^{12}\text{C}, ^{12}\text{N}$ ) AND ( $^{12}\text{C}, ^{12}\text{B}$ ) REACTIONS AT E/A = 70 MeV

N. Anantaraman, J.S. Winfield, Sam M. Austin, E. Adamides, C. Djalali, J.A. Nolen Jr.,  
A. Gillibert<sup>a</sup>, Z.W. Long<sup>a</sup> and W. Mittig<sup>a</sup>

A study of the heavy-ion charge exchange reaction  $^{12}\text{C}(^{12}\text{C}, ^{12}\text{N})^{12}\text{B}$  at 35 MeV/nucleon at MSU concluded that two-step processes dominated at that energy, but that they should become negligible compared to the one-step process at energies > 50-60 MeV/nucleon.<sup>1</sup> Under this circumstance, the quantum numbers of the projectile and ejectile enforce  $\Delta S = \Delta T = 1$ ; then the ( $^{12}\text{C}, ^{12}\text{N}$ ) reaction becomes a tool to study spin excitations, and in particular Gamow-Teller  $\beta^+$  strengths, in nuclei.

To verify this expectation and for use as a spectroscopic tool, the ( $^{12}\text{C}, ^{12}\text{N}$ ) reaction was studied on targets of  $^{12}\text{C}$  and  $^{54,56,58}\text{Fe}$  at an energy of 70 MeV/nucleon at Laboratoire GANIL. Determination of Gamow-Teller  $\beta^+$  strengths for low-lying levels in the Mn nuclei is important in connection with outstanding unresolved problems in astrophysics (rates of evolution of stars toward and through the supernova stage) and in nuclear physics (the quenching of Gamow-Teller strength in nuclei). To calibrate the reaction as a spin probe, ( $^{12}\text{C}, ^{12}\text{B}$ ) data were taken on  $^{12}\text{C}$ ,  $^{26}\text{Mg}$ ,  $^{54}\text{Fe}$ ,  $^{58}\text{Ni}$  and  $^{90}\text{Zr}$ , for transitions to states with known Gamow-Teller strengths (from  $\beta$ -decay for the first two targets and from (p,n) reactions for the last three).

Self-supporting targets, of thickness about  $1 \text{ mg/cm}^2$  except for carbon ( $0.48 \text{ mg/cm}^2$ ), were bombarded with the 70 MeV/nucleon  $^{12}\text{C}$  beam of the GANIL facility. The outgoing particles were detected and identified in the magnetic spectrometer SPEG.<sup>2</sup> Momentum and scattering angle were obtained by reconstruction of the trajectories in the focal plane. The detection system consisted of: i) two position-sensitive drift chambers, each one giving two position (x

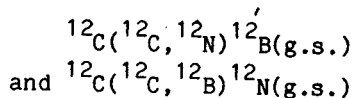
and y) signals, located on either side of the focal plane, to determine the scattering angle and the magnetic rigidity of the detected particles; ii) an ionization chamber, to measure the energy loss of the outgoing particles; iii) a plastic scintillator, to measure the total energy and to provide the start signal of the time of flight, for which the stop signal was obtained from the RF of the last cyclotron. All the gas counters were filled with isobutane.

The angular acceptance of the spectrometer in the horizontal reaction plane covered  $-0.5^\circ$  to  $+3.5^\circ$  for the ( $^{12}\text{C}, ^{12}\text{N}$ ) reaction on all targets; for  $^{56}\text{Fe}$ , data from  $3^\circ$  to  $7^\circ$  were also obtained. For the ( $^{12}\text{C}, ^{12}\text{B}$ ) reaction, the observed angular range was  $-3.7^\circ$  to  $+0.3^\circ$ . The vertical acceptance was about  $0.5^\circ$  for both reactions. The choices for the horizontal angular ranges were constrained by the (fixed) locations of the Faraday cups available to stop the beam. During the analysis, the angular range was subdivided into bins corresponding to horizontal angular acceptances of typically  $0.16^\circ$ .

Data obtained with an angle-calibration mask proved to be impossible to interpret; it is conjectured that they were vitiated as the result of a beam profiler probably left in the path of the beam. The angle calibration was, therefore, obtained initially by comparing the observed shift in the x-position of the peak from the  $\text{H}(^{12}\text{C}, ^{12}\text{N})\text{n}$  reaction with the expected kinematic energy shift as a function of angle. (Hydrogen was present as a contaminant in all the targets and was a constituent of the  $(\text{C}_3\text{H}_6)_\text{n}$  (polypropylene) target that was also studied.) The determination of  $0^\circ$  was made in four ways: from the maximum in the angular distributions

for the ( $^{12}\text{C}, ^{12}\text{N}$ ) reaction on C, on H in the C target, and on H in the ( $\text{C}_3\text{H}_6$ )<sub>n</sub> target, and from the maximum energy for the reaction on H (highest x-position). All these agreed to within  $0.1^\circ$ . This angle calibration was then checked by extracting  $^{12}\text{C}$  elastic scattering angular distributions for  $^{26}\text{Mg}$ ,  $^{54}\text{Fe}$  and  $^{90}\text{Zr}$ , and comparing them (in both magnitude and shape) with optical model predictions. The agreement in shape was quite good, again to within  $0.1^\circ$  (lab). Thus the angular accuracy is estimated to be better than  $\pm 0.1^\circ$ .

The absolute normalization of the cross sections was obtained from the target thickness and the integrated beam current measured in the various Faraday cups. A simple check on the consistency of this method is provided by the requirement that the cross sections for the two mirror reactions,



should be identical. However, we find that, while the shapes of the angular distributions for the two reactions are indeed similar, the second has a cross section higher by about 60% than the first. The reason for this has not yet been found.

Figure 1 compares the spectra from the ( $^{12}\text{C}, ^{12}\text{N}$ ) and ( $^{12}\text{C}, ^{12}\text{B}$ ) reactions on  $^{12}\text{C}$ . Several differences are evident. The energy resolution for the first reaction is about 280 keV ( $\Delta E/E = 3.3 \times 10^{-4}$ ), and about 550 keV for the second. These values are typical for the two reactions on all the targets studied. The difference can be accounted for if the resolution is determined by the signal to noise ratio in the drift chambers; the energy loss for boron is about half that for nitrogen ( $5^2/7^2$ ).

The other differences in the spectra are partly due to the different level spacings in the two final nuclei, and partly due to the

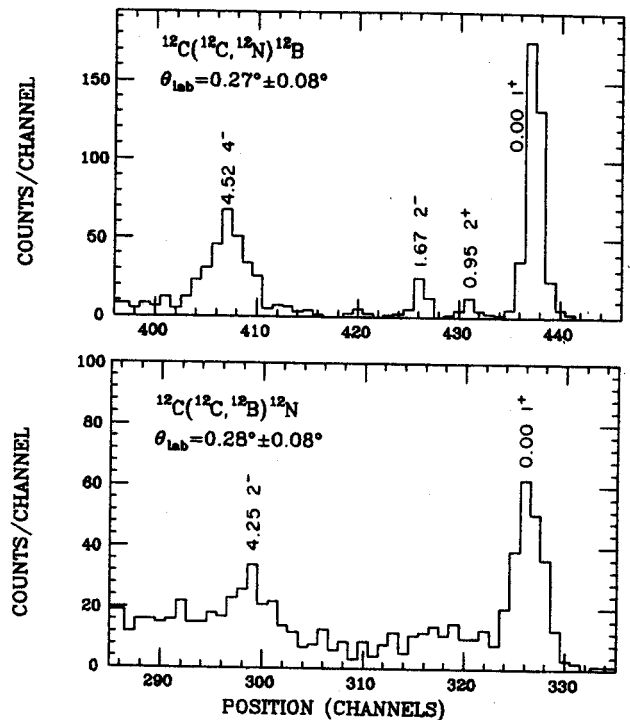


Fig. 1: Spectra of the ( $^{12}\text{C}, ^{12}\text{N}$ ) and ( $^{12}\text{C}, ^{12}\text{B}$ ) reactions measured on  $^{12}\text{C}$  at  $E/A = 70$  MeV.

additional population of excited bound states in the case of the ejectile  $^{12}\text{B}$ . These two reactions have also been studied at the same bombarding energy by another group at GANIL.<sup>3</sup>

Figure 2 shows the angular distribution measured for the  $^{12}\text{C}(^{12}\text{C}, ^{12}\text{N})^{12}\text{B}(\text{g.s.})$  reaction, along with a one-step microscopic distorted-wave Born approximation (DWBA) calculation using the code SESIME.<sup>4</sup> The optical potential for the distorted waves was taken from the results of 84 MeV/nucleon  $^{12}\text{C} + ^{12}\text{C}$  elastic scattering [potential F of Ref. 5]. Only the  $V_{\sigma\tau}$  part of the central nucleon-nucleon interaction was included in the form factor; a Yukawa shape with a range of 1 fm was used for it. The tensor and exchange terms were not considered. The required strength of  $V_{\sigma\tau}$  to fit the data as shown is 13.0 MeV. If the 40%-lower cross section measured for the mirror ( $^{12}\text{C}, ^{12}\text{B}$ ) reaction proves to be the correct one, the extracted value of  $V_{\sigma\tau}$  would be 10.4 MeV. The fit to the angular distribution is not good. Calculations which include the tensor and

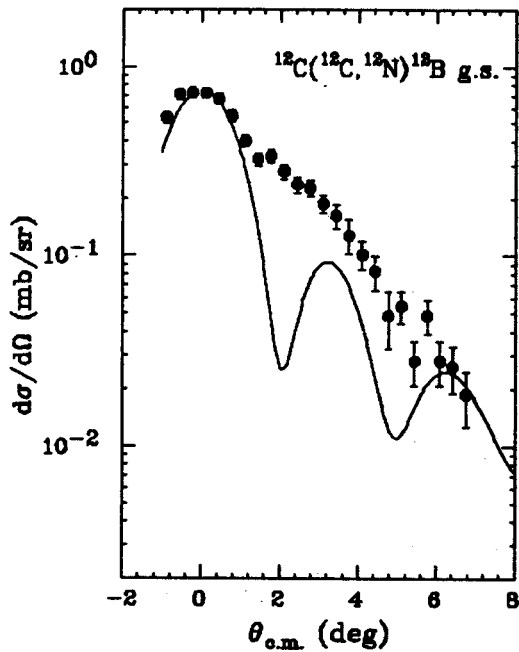


Fig. 2: Angular distribution for the  $^{12}\text{C}(^{12}\text{C}, ^{12}\text{N})^{12}\text{B}(\text{g.s.})$  reaction at  $E/A = 70$  MeV. The curve is the result of a calculation described in the text.

exchange terms are in progress,<sup>6</sup> to see if the pronounced oscillations in the calculated angular distribution will be washed out, as was observed for the ( $^6\text{Li}, ^6\text{He}$ ) reaction.<sup>7</sup>

Figure 3 shows the ( $^{12}\text{C}, ^{12}\text{B}$ ) spectra measured with different targets. Yields for the low-lying  $1^+$  states, which are of interest for the calibration of this reaction as a spin probe, were obtained using a peak-fitting program. The fact that states of other multipolarities are excited as strongly as  $1^+$  states, even at angles close to  $0^\circ$ , shows that the reaction is not selective of  $\Delta L=0$  transitions. The  $1^+$  states of interest are:

$$^{12}\text{C} \rightarrow ^{12}\text{N}: E_x = 0.00 \text{ MeV}, B(\text{GT}) = 0.94 \pm 0.006$$

$$^{26}\text{Mg} \rightarrow ^{26}\text{Al}: E_x = 1.06 \text{ MeV}, B(\text{GT}) = 1.21 \pm 0.05$$

$$^{54}\text{Fe} \rightarrow ^{54}\text{Co}: E_x = 0.94 \text{ MeV}, B(\text{GT}) = 0.73 \pm 20\%$$

$$^{58}\text{Ni} \rightarrow ^{58}\text{Cu}: E_x = 1.05 \text{ MeV}, B(\text{GT}) = 0.50 \pm 20\%$$

$$^{90}\text{Zr} \rightarrow ^{90}\text{Nb}: E_x = 2.3 \text{ MeV}, B(\text{GT}) = 1.80 \pm 20\%$$

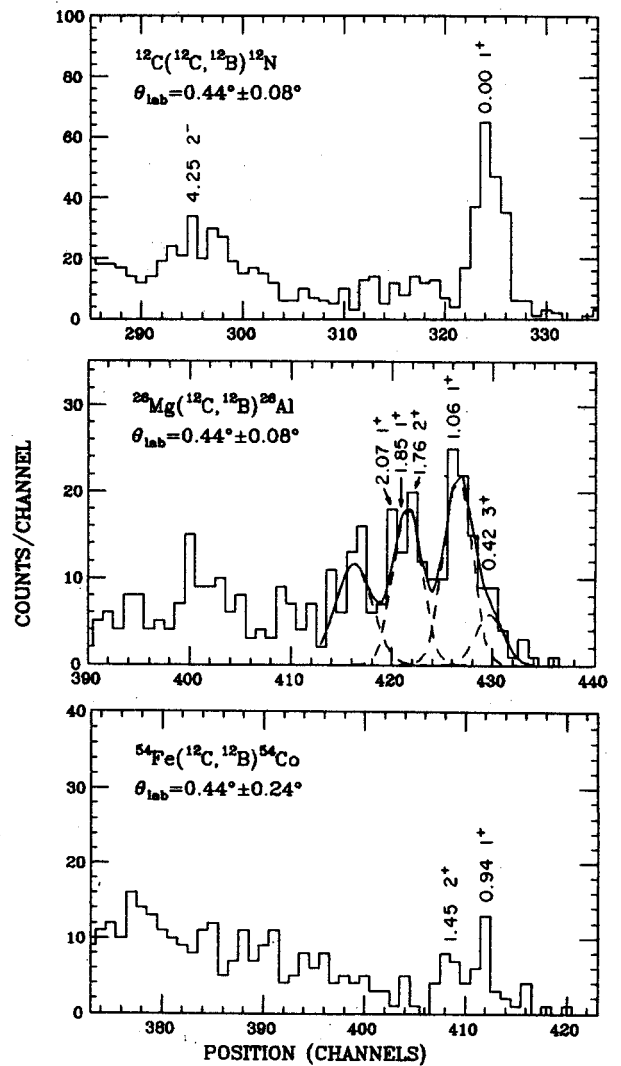


Fig. 3: Spectra of the ( $^{12}\text{C}, ^{12}\text{B}$ ) reaction on various targets at  $E/A = 70$  MeV.

The data for the two heaviest targets are still under analysis.

The ratio of the cross section at  $\theta_{\text{lab}} = 0.28^\circ$  to  $B(\text{GT})$  shows a marked decrease with  $A$ . This behavior is analogous to that found for the ( $p, n$ ) reaction<sup>8</sup> at  $E_p = 100-200$  MeV but is unlike the nearly constant ratio found for the ( $^6\text{Li}, ^6\text{He}$ ) reaction<sup>7</sup> at  $E/A = 25-35$  MeV. This result is preliminary. If our further analysis, including DWBA calculations, confirms the validity of such a trend, a plot of the ratio vs.  $A$  may be viewed as a calibration curve not only for ( $^{12}\text{C}, ^{12}\text{B}$ ) but also, after small corrections, for ( $^{12}\text{C}, ^{12}\text{N}$ ) at 70 MeV/nucleon.

Figure 4 shows the ( $^{12}\text{C}, ^{12}\text{N}$ ) spectrum for the  $^{56}\text{Fe}$  target. The tentative identification of the peaks at 0.11 MeV and 1.17 MeV excitations as  $1^+$  states is based on results from low-energy  $^{56}\text{Fe}(t, ^3\text{He})$  work, where they are the two strongest  $1^+$  states and have roughly the same relative strength as observed by us.<sup>9</sup> The ( $t, ^3\text{He}$ ) study finds additional  $1^+$  states at excitations up to 3 MeV; they may be present in our spectrum as well. Analysis of the ( $^{12}\text{C}, ^{12}\text{N}$ ) data is in progress.

a. Laboratoire GANIL, Caen, France.

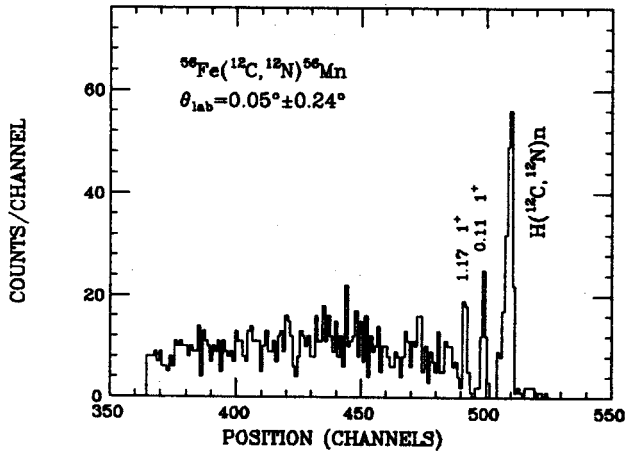


Fig. 4: Spectrum of  $^{56}\text{Fe}(^{12}\text{C}, ^{12}\text{N})^{56}\text{Mn}$  at  $E/A = 70$  MeV.

## References

1. J.S. Winfield, N. Anantaraman, S.M. Austin, L.H. Harwood, J. van der Plicht, H.-L. Wu and A.F. Zeller, Phys. Rev. C 33, 1333 (1986); C 35, 1166 (1987) [E].
2. J. Gastebois, in "Detectors in Heavy-Ion Reactions", edited by W. von Oertzen (Springer-Verlag, Berlin, 1983), p. 126.
3. W. von Oertzen, Invited Talk at First Topical Meeting on Giant Resonance Excitation in Heavy-Ion Collisions, Legnaro, Italy (1987).
4. A. Etchegoyen, D. Sinclair, S. Liu, M.C. Etchegoyen, D.K. Scott and D.L. Hendrie, Nucl. Phys. A397, 343 (1983).
5. M. Buenerd, A. Lounis, J. Chauvin, D. Lebrun, P. Martin, G. Duhamel, J.C. Gondrand and P. de Saintignon, Nucl. Phys. A424, 313 (1984).
6. H. Lenske, priv. comm. (1988); J.A. Carr, priv. comm. (1988).
7. J.S. Winfield, N. Anantaraman, S.M. Austin, Z. Chen, A. Galonsky, J. van der Plicht, H.-L. Wu, C.C. Chang and G. Ciangaru, Phys. Rev. C 35, 1734 (1987).
8. C.D. Goodman, C.A. Goulding, M.B. Greenfield, J. Rapaport, D.E. Bainum, C.C. Foster, W.G. Love and F. Petrovich, Phys. Rev. Lett. 44, 1755 (1980).
9. F. Ajzenberg-Selove, R.E. Brown, E.R. Flynn and J.W. Sunier, Phys. Rev. C 30, 1850 (1984); C 31, 777 (1985).

MASS OF  $^{39}\text{Sc}$  VIA THE  $^{40}\text{Ca}(^7\text{Li}, ^8\text{He})$  REACTION

M.F. Mohar, E. Adamides, W. Benenson, C. Bloch, B.A. Brown, J. Clayton, E. Kashy, M. Lowe, J.A. Nolen Jr., W.E. Ormand, J. van der Plicht, B. Sherrill, J. Stevenson, and J.S. Winfield

The proton unbound nucleus  $^{39}\text{Sc}$  was observed for the first time, and its ground state mass was determined via the Q-value measurement of the  $^{40}\text{Ca}(^7\text{Li}, ^8\text{He})^{39}\text{Sc}$  reaction<sup>1,2</sup>. From its mass, we deduce that  $^{39}\text{Sc}$  is 633(42) keV proton unbound, and, therefore, it is just over the proton drip line. This result is important for determining whether  $^{39}\text{Sc}$  is a candidate for measurable ground state proton radioactivity.

The ground state of  $^{39}\text{Sc}$  is the third known member of the A=39 isobaric quartet, and hence its mass can be used to determine the b and c coefficients in the Isobaric Multiplet Mass Equation (IMME)<sup>3</sup> if the assumption of a quadratic form for this equation is made. The A=39 coefficients are compared to systematics and the predictions of the isospin-nonconserving Hamiltonian formulation of Ormand and Brown.<sup>4</sup> In general, the  $^{39}\text{Sc}$  results provide a comparison for nuclear structure calculations which involve both the sd and f shells and are a good test for the extrapolation of various mass formulae beyond the proton drip line.

The ( $^7\text{Li}, ^8\text{He}$ ) reaction on a  $^{40}\text{Ca}$  target was measured using an E/A=27.24(5) MeV  $^7\text{Li}^{2+}$  beam from the K500 cyclotron, and the reaction products were detected in the S320 spectrometer.<sup>2</sup> The reaction was measured at an angle of 4.80(6) degrees, and a nominal dipole field of 14.8770 kG. The  $^8\text{He}$  ions were identified by a combination of TOF in the spectrograph,  $\Delta E$  in the ion chambers, and light output from the plastic scintillator. Although the  $^8\text{He}^{2+}$  and  $^4\text{He}^{1+}$  ions overlap in the  $\Delta E$  - TOF spectrum, they are clearly resolved with the light output signal from the stopping plastic scintillator since  $^4\text{He}^{1+}$  ions have only half the

energy of the  $^8\text{He}^{2+}$  ions of the same rigidity. A potential problem with this reaction is the very high rate of tritons from  $^7\text{Li} \rightarrow t + \alpha$  breakup. However, a hardware TOF gate allowed the rejection of tritons.

The position spectra for the  $^{40}\text{Ca}(^7\text{Li}, ^8\text{He})^{39}\text{Sc}$  reaction is shown in Fig. 1. The overall resolution was 240 keV FWHM. Using mass excesses from Wapstra and Audi<sup>5</sup>, we calculate the Q-value of the  $^{40}\text{Ca}(^7\text{Li}, ^8\text{He})^{39}\text{Sc}$  reaction to be -37.40(4) MeV. The corresponding  $^{39}\text{Sc}$  mass excess is -14.14(4) MeV. The error is found by directly adding the average systematic error from the calibration (15 keV) to the statistical error in the ground state  $^{39}\text{Sc}$  position peak (26 keV). The measured  $^{40}\text{Ca}(^7\text{Li}, ^8\text{He})^{39}\text{Sc}$  cross section at 191 MeV and 4.8 degrees is 70(30) nb/sr.

The  $^{39}\text{Sc}$  mass excess determined in this experiment is compared to various models in Table I. In general, the agreement is similar to that expected from the overall accuracy of

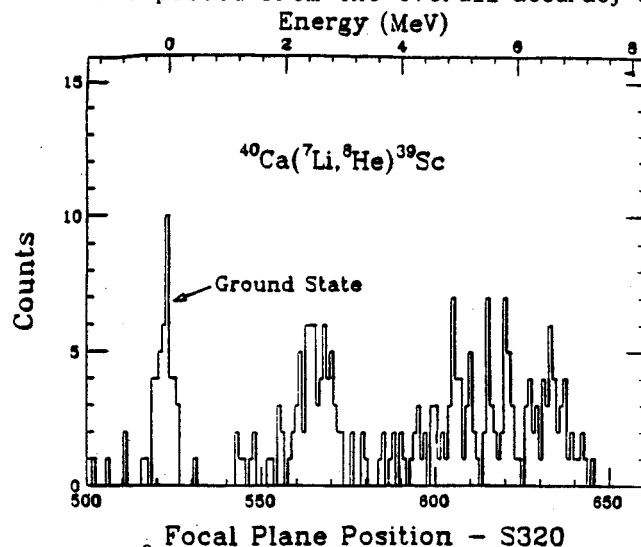


Fig. 1:  $^8\text{He}$  position spectrum at the focal plane of the S320 spectrometer for the  $^{40}\text{Ca}(^7\text{Li}, ^8\text{He})^{39}\text{Sc}$  reaction.

the predictions<sup>6</sup>. It is interesting that Moller-Nix predict that <sup>39</sup>Sc should be proton unbound by only 40 keV. If this had been true, then <sup>39</sup>Sc would be a candidate for long lived proton decay, or perhaps for decay by branching to both protons and  $\beta^+$  emission. However, given the fact that the present experiment finds that the proton is unbound by 633(42) keV, one can estimate that the lifetime is on the order of  $4 \times 10^{-13}$  seconds. This estimation was carried out by calculating the barrier penetration for an l=3 proton through a barrier with  $R=1.2A^{1/3}$  fm. The calculated spectroscopic factor in the  $0d_{3/2}-0f_{7/2}$  model space<sup>7</sup> is 0.90. Therefore, <sup>39</sup>Sc does not seem to be a candidate for proton decay with a lifetime comparable to that of beta decay.

Table I. Predictions of the mass excess of <sup>39</sup>Sc, and the result from this work.

MODEL <sup>a</sup>	VALUE (MeV)
MYERS	-15.85
GROOTE HILF TAKAHASHI	-15.73
LIRAN ZELDES	-13.98
BEINER LOMBARD MAS	-13.6
JANECKE GARVEY KELSON	-14.07
WAPSTRA	-14.18
MOLLER <sup>b</sup> NIX	-14.72
EXPERIMENT	-14.14 (4)

- a. S. Maripuu Spec. Ed., 1975 Mass Predictions, At. Nucl. Data Tables, 17, 411 (1976).  
 b. P. Moller and J.R. Nix, Atomic Data and Nuclear Data Tables, 26, 165 (1981).

The measured mass of <sup>39</sup>Sc also allows the b and c coefficients of the IMME to be extended to the A=39, T=3/2 isobaric quartet ( $BE = a + bT_Z + cT_Z^2 + dT_Z^3 + \dots$ ), under the very well established assumption that the d-coefficient of the IMME can be set to zero.<sup>3</sup> From the two other known members of the quartet, <sup>39</sup>Ar(g.s.,  $ME = -33.242(5)$  MeV)<sup>5</sup> and the T=3/2,  $J^\pi = 7/2^-$  state in <sup>39</sup>K ( $ME = -27.261(2)$  MeV)<sup>5,8</sup>, we obtain the results given in Table II. These are compared to systematic trends in Fig. 2. Also included in Table II are the corresponding b and c coefficients predicted by the recent empirical isospin-nonconserving (INC) Hamiltonian developed for the  $0d_{3/2}-0f_{7/2}$  shell-model space by Ormand and Brown. In that work, Hamiltonians were developed for the purpose of calculating INC processes and were determined empirically under the requirement that the parameters of a Coulomb plus phenomenological isovector and isotensor potential reproduce experimental b and c coefficients. For the  $0d_{3/2}-0f_{7/2}$  space<sup>7</sup>, 22 b coefficients, including 3 from T=1 doublets in the A=39 system, and 14 c-coefficients were fit. An rms deviation of approximately 21 keV was

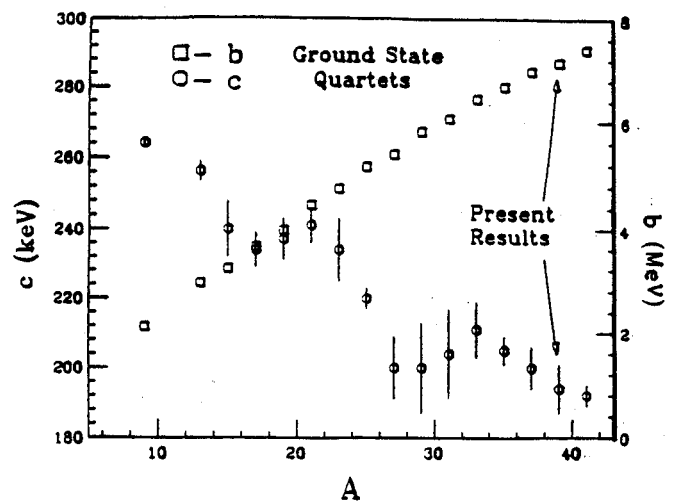


Fig. 2: b and c coefficients from the Isobaric Multiplet Mass Equation for ground state quartets. (W. Benenson and E. Kashy, Rev. Mod. Phys. 51, 527 (1979); M.S. Antony et al., Atomic and Nuclear Data Tables, 33, 457 (1985).

Table II: b and c coefficients for the A=39 quartet using the experimental mass of  $^{39}\text{Sc}$  and using the INC formalism of Ormand and Brown.

	<u>b (MeV)</u>	<u>c (keV)</u>
Experimental	7.150(14)	194(7)
INC Calculation	7.154(21)	207(21)

obtained for both. The resulting Hamiltonian contained a small charge-asymmetric interaction in which the neutron-neutron two-body interaction was approximately 1.8% more attractive than the proton-proton interaction, and a short-range charge-dependent interaction in which the proton-neutron interaction was 2.4% more attractive than the average of the proton-proton and neutron-neutron interactions. Aside from being able to calculate the extent to which isospin conservation is violated, the empirical Hamiltonian can also be used to predict other isobaric mass shifts as is shown by the good agreement between the experimental and predicted values. The excellent agreement of the INC calculations with the results from our experiment indicate the good predictive power of the INC formulation.

In conclusion, the  $^{40}\text{Ca}(^7\text{Li}, ^8\text{He})$  reaction has been used to measure the mass excess of  $^{39}\text{Sc}$  as  $-14.14(4)$  MeV. This value agrees within the uncertainties of the various mass models. From the mass excess, we have estimated that the ground-state proton decay of  $^{39}\text{Sc}$  has a lifetime of  $4 \times 10^{-13}$  seconds. The ground state mass measurement also allows the b and c coefficient systematics for isobaric quartets to be extended to A=39, and the results are in very good agreement with the Ormand-Brown INC shell-model predictions.

#### References

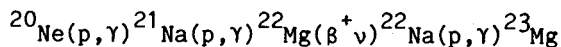
1. E. Stiliaris et al., Z. Phys. A326, 139 (1987).
2. B. Sherrill, Doctoral Dissertation, Michigan State University, 1985; B. Sherrill et al., Phys. Rev. C 31, 875 (1985).
3. W. Benenson and E. Kashy, Rev. Mod. Phys. 51, 527 (1979).
4. W.E. Ormand and B.A. Brown, to be published, NBI-87-63.
5. A.H. Wapstra and G. Audi, 1983 Atomic Mass Table, Nucl. Phys. A432, 1 (1985).
6. S. Maripuu Spec. Ed., 1975 Mass Predictions, At. Nucl. Data Tables 17, 411 (1976).
7. S.T. Hsieh et al., Proceedings of the AIP Conference on Nuclear Structure at High Spin, Excitation, and Momentum Transfer, ed. by H. Nann (Am. Inst. of Physics, New York, 1986) p. 357; Bull. of the American Physical Society 30, 731 (1985).
8. P.M. Endt and C. Van Der Leun, Nucl. Phys. A310, 517 (1978).



M. Wiescher<sup>a</sup>, M. Mohar, B.A. Brown, J. Görres<sup>a</sup>, B. Sherrill, and J.S. Winfield

### Introduction

The production of  $^{22}\text{Na}$  in the hot hydrogen burning in novae, supernovae or massive stars has been discussed by numerous authors.<sup>1,2</sup> It is thought to be produced in substantial quantities in the hot Ne-Na-cycle by:



This reaction sequence will occur at temperature and density conditions where the  $^{21}\text{Na}(p,\gamma)$  reaction is expected to proceed more rapidly than the competing  $\beta$ -decay ( $T_{1/2}=22.48$  sec).<sup>3</sup> At these temperatures, however, proton capture on  $^{22}\text{Mg}$  ( $T_{1/2}=3.86$  sec),  $^{22}\text{Mg}(p,\gamma)^{23}\text{Al}$ , may also occur. Due to the low Q-value of the reaction,  $Q = 0.127$  MeV, at high temperatures the photodisintegration of  $^{23}\text{Al}$ ,  $^{23}\text{Al}(\gamma,p)^{22}\text{Mg}$ , will prevent a substantial production of  $^{23}\text{Al}$  after the equilibrium has been reached. The abundance ratio depends on the temperature  $T_9$  (in  $10^9$  K), the density  $\rho(\text{g/cm}^3)$  and the mass fraction of hydrogen  $X(\text{H})$ :

$$\frac{n(^{23}\text{Al})}{n(^{22}\text{Mg})} = 3.25 \cdot 10^{-10} \cdot T_9^{3/2} \cdot \rho \cdot X(\text{H}) \cdot \exp(1.474/T_9)$$

and is independent of the proton capture reaction rate of  $^{22}\text{Mg}(p,\gamma)^{23}\text{Al}$ .

However, in explosive events, triggering the rp-process<sup>4</sup> in novae, accreting neutron stars and black holes<sup>5</sup>, the timescales involved may be too short to reach the equilibrium between proton capture on  $^{22}\text{Mg}$  and photodisintegration of  $^{23}\text{Al}$ . The production or depletion of  $^{22}\text{Mg}$  depends largely on the original abundances  $[N_i]$ , the capture rates  $\lambda_{i,1}$ , and the rates for the  $\beta$ -decay  $\lambda_{i\beta}$  and the photodisintegration  $\lambda_{i\gamma}$ :

$$\begin{aligned} \frac{d}{dt} [^{22}\text{Mg}] = & -\lambda_{22.1} \cdot [^{22}\text{Mg}][\text{H}] - \lambda_{22\beta} \cdot [^{22}\text{Mg}] \\ & + \lambda_{21.1} \cdot [^{21}\text{Na}][\text{H}] + \lambda_{23,\gamma} [^{23}\text{Al}] \end{aligned}$$

The current proton capture rates for  $^{21}\text{Na}(p,\gamma)^{22}\text{Mg}$  and  $^{22}\text{Mg}(p,\gamma)^{23}\text{Al}$  are estimated mainly on the basis of nuclear structure information of the particular compound nuclei.<sup>3,6</sup>

However, the rate of  $^{22}\text{Mg}(p,\gamma)^{23}\text{Al}$  is still very uncertain.<sup>6</sup> Due to the low proton threshold  $Q$ , the reaction rate will be determined by the nonresonant f-wave direct capture to the ground state and by the s-wave resonant capture to the first excited state in  $^{23}\text{Al}$ . The resonant part of the rate depends exponentially on the resonance energy and linearly on its resonance strength  $\omega\gamma$ , neither of which is known. The mirror level in  $^{23}\text{Ne}$  has an excitation energy of 1.02 MeV<sup>7</sup>, its pronounced single particle structure suggests a large Thomas Ehrman shift between the mirror states. This indicates that the resonance in  $^{22}\text{Mg}(p,\gamma)^{23}\text{Al}$  may contribute at significantly lower energies than suggested before.<sup>4,6</sup>

In the present work we will describe an experiment to determine the excitation energy of the first excited state in  $^{23}\text{Al}$  and will discuss its implications for the reaction rate of  $^{22}\text{Mg}(p,\gamma)^{23}\text{Al}$ .

### Experimental procedure and analysis

We measured the reaction  $^{24}\text{Mg}(^7\text{Li}, ^8\text{He})^{23}\text{Al}$  to determine the level energy of the first excited state in  $^{23}\text{Al}$ . An enriched  $^{24}\text{Mg}$  target ( $6.25\text{mg/cm}^2$ ) was bombarded with a 191 MeV  $^7\text{Li}$  beam from the K500 cyclotron. The reaction particles were detected in the focal plane of the S-320 spectrometer.<sup>8</sup>

Figure 1 shows the spectrum obtained from the  $^{24}\text{Mg}(^7\text{Li}, ^8\text{He})^{23}\text{Al}$  reaction. The ground state in  $^{23}\text{Al}$ ,  $J^\pi=5/2^+$ , is strongly populated,  $\sigma=0.7(4)$   $\mu\text{b}/\text{sr}$ ; the spectrum indicates also strong transitions to unresolved levels between 2.5 and 3.7 MeV excitation energy. The transition to the first excited state in  $^{23}\text{Al}$ ,  $J^\pi=1/2^+$ , could be identified as a pronounced shoulder,  $\sigma=0.2(1)$   $\mu\text{b}/\text{sr}$ , on the low energy side of the ground state peak by applying the peak shape from the ground state transition in  $^{40}\text{Ca}(^7\text{Li}, ^8\text{He})^{39}\text{Sc}$  (see Fig. 1). This results in an excitation energy of  $E_x = 460 \pm 60$  keV. This result agrees also with a previous study of  $^{23}\text{Al}$  by  $^{28}\text{Si}(^3\text{He}, ^8\text{Li})^{23}\text{Al}$  at bombarding energies of 76.3 MeV.<sup>9</sup> The measured spectrum (resolution 150 keV) indicates a weak peak, shown in Fig. 2 of ref. 9, but not assigned by those authors. In the light of the present data, this peak can be assigned to the transition to the first excited state in  $^{23}\text{Al}$ . Reanalysis yields an excitation energy of  $E_x=475 \pm 50$  keV, well in agreement with the present results.

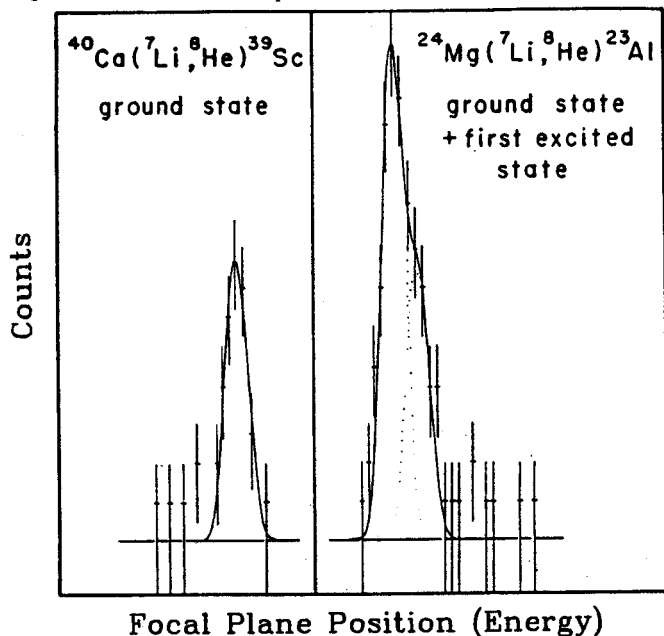


Fig. 1: Analysis of the transitions to the ground state and the first excited state in  $^{23}\text{Al}$ . Peak shape parameters were obtained from the ground state transition in  $^{40}\text{Ca}(^7\text{Li}, ^8\text{He})^{39}\text{Sc}$  measured at equal experimental conditions.

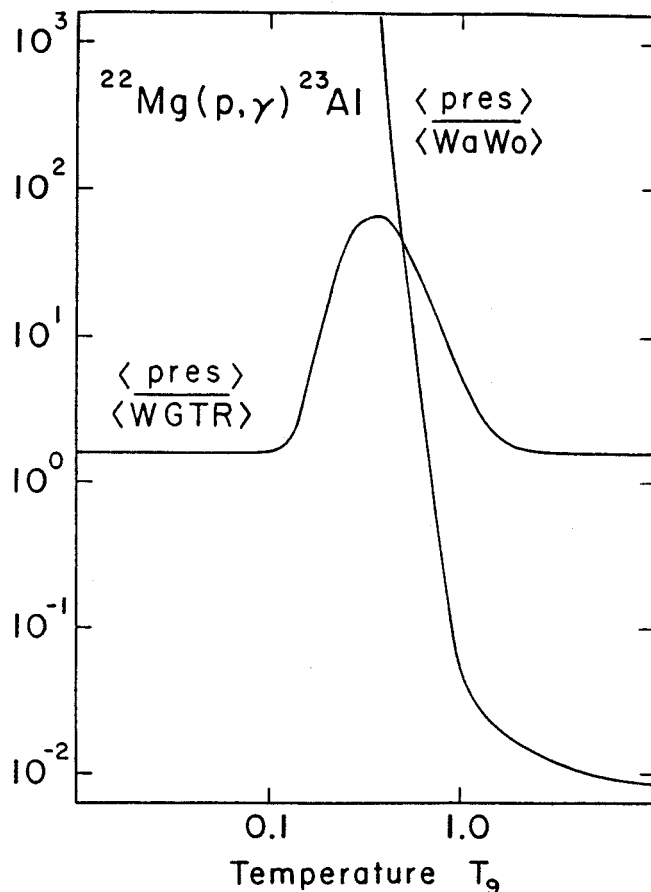


Fig. 2: The present total reaction rate of  $^{22}\text{Mg}(p,\gamma)^{23}\text{Al}$  in comparison with previous estimates<sup>4,6</sup>.

The measurement of the excitation energy of the first excited state in  $^{23}\text{Al}$ ,  $J^\pi=1/2^+$ ,  $T=3/2$ , in combination with the known excitation energies of the  $T=3/2$  analog states in  $^{23}\text{Na}$  and  $^{23}\text{Ne}$ <sup>7</sup>, allows the computation of the Isobaric Mass Multiplet Equation (IMME) coefficients for the first excited  $A=23$  isospin quartet. Table I shows the derived parameter in comparison with the IMME coefficients for the  $T=3/2$  ground state quartet.<sup>10</sup> Also included in Table I are the  $A=23$   $J^\pi=5/2^+$ ,  $1/2^+$   $b$  and  $c$  coefficients obtained with the recent empirical isospin-nonconserving (INC) interaction of Ormand and Brown.<sup>11</sup> The ground state ( $J^\pi=5/2^+$ ) experimental values agree reasonably well with those calculated; however the  $b$  and  $c$  coefficients obtained from the excited state ( $J^\pi=1/2^+$ ) are not in good agreement. As explained by Ormand and Brown for

Table I

Coefficients of the isobaric multiplet mass equation (in MeV) for the ground state and first excited state A=23 isobaric quartet.

A	$J^\pi$	b	c	Ref.
23	$5/2^+$	$-3.973 \pm 0.008$	$0.230 \pm 0.004$	<sup>10)</sup>
		-3.924	0.255	INC
23	$1/2^+$	$-3.789 \pm 0.022$	$0.259 \pm 0.010$	pres
		-3.913	0.221	INC

the similar case of A=17, since the Ormand-Brown interaction is based on harmonic oscillator wave functions this deviation is most likely a result of the small binding energy of the  $1s_{1/2}$  proton states, which results in a large rms charge radius and a smaller Coulomb energy.

The weighted average of the present result and that of Benenson et al.<sup>9</sup> yields an excitation energy of  $E_x = 470 \pm 40$  keV, which corresponds to a resonance energy in  $^{22}\text{Mg}(p,\gamma)^{23}\text{Al}$  of  $E_r^{\text{lab}} = 360 \pm 40$  keV. This is significantly lower than previously suggested.<sup>6</sup> A complete discussion of the rate calculations can be found in the article by Wiescher, et al. from this work; however, in Fig. 2 we compare the present results with previous suggestions for the rate of  $^{22}\text{Mg}(p,\gamma)^{23}\text{Al}$ .<sup>4,6</sup> The large discrepancies with ref. 4 at low temperatures results from the neglect of the direct capture and are discussed in ref. 6. Compared to the rate of ref. 6 the new rate shows a slight enhancement at temperatures  $0.1 \leq T_9 \leq 1.0$ , due to the significantly lower resonance energy.

The reaction rate contributions are shown in Fig. 3. The shaded area indicates the lower and upper limit for the resonance rate caused by the uncertainties in resonance energy and resonance strength. In the temperature range  $T_9 = 0.1$  to 1.0, the resonant part dominates clearly the rate, while at higher temperatures, the direct capture is more influential due to the lack of high energy resonances.

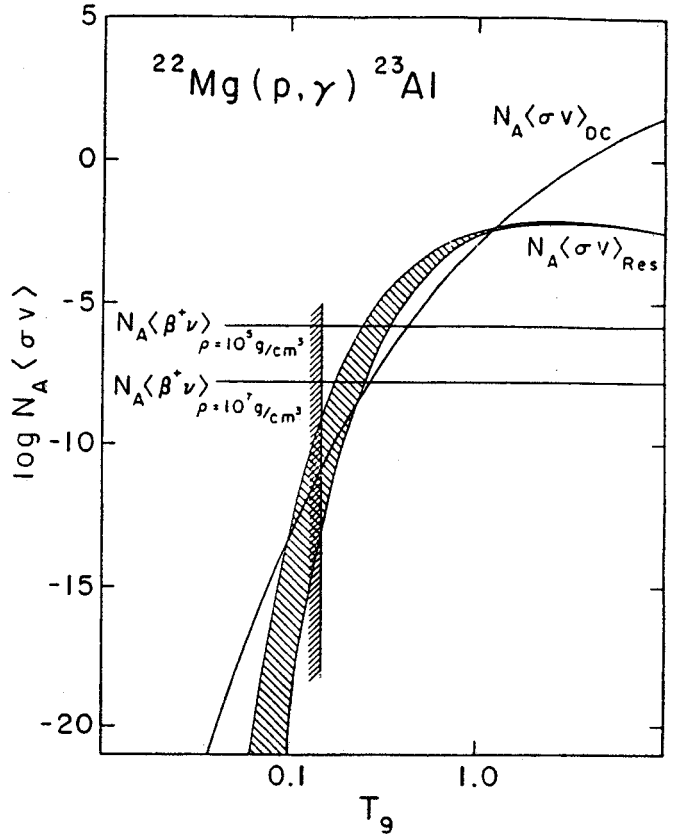


Fig. 3: Shown is the resonant and nonresonant reaction rate of  $^{22}\text{Mg}(p,\gamma)^{23}\text{Al}$ . The shaded area in the resonant contribution indicates the uncertainty due to the uncertainty of the level energy. The shaded bar at  $T_9 = 0.15$  marks the temperature range where  $^{22}\text{Mg}$  will be produced by  $^{21}\text{Na}(p,\gamma)^{22}\text{Mg}^3$ . Also shown for comparison are the  $\beta$ -decay rates of  $^{22}\text{Mg}$  (in units  $\text{cm}^3 \text{mole}^{-1} \text{sec}^{-1}$ ) for two different densities, where the decay rate scales linearly with the density.

The shaded line marks the stellar temperature above which  $^{22}\text{Mg}$  will be produced in significant amounts by the reaction  $^{21}\text{Na}(p,\gamma)^{22}\text{Mg}^3$ . Indicated is also the  $\beta$ -decay rate (in units  $\text{cm}^3 \text{mole}^{-1} \text{s}^{-1}$ ) of  $^{22}\text{Mg}$  for two different densities  $\rho = 10^5$  and  $10^7 \text{ g/cm}^3$ , which are typically assumed in explosive environments. This suggests that at nova conditions,  $T_9 \leq 0.5$ ,  $\rho = 10^3 - 10^5 \text{ g/cm}^3$ , no break out via the  $(p,\gamma)$  reaction will occur and the material, processed by  $^{21}\text{Na}(p,\gamma)^{22}\text{Mg}$  (for  $T_9 > 0.2^3$ ), will decay to  $^{22}\text{Na}$ . On accreting neutron stars, at high

temperatures beyond  $T_9=0.4$  and densities<sup>5</sup>  $\rho > 10^6 \text{g/cm}^3$ , the  $(p,\gamma)$  rate exceeds sufficiently the competing  $\beta$ -decay rate; in the short timescales of the thermal runaway, before equilibrium with the inverse photodisintegration will take place, significant amounts of  $^{22}\text{Mg}$  will be processed towards higher mass isotopes. More detailed reaction network calculations are necessary to analyze quantitatively the reaction flow at different temperature and density conditions.

---

a. University of Notre Dame, Notre Dame, Indiana, 46556

#### References

1. D.D. Clayton, F. Hoyle, Ap. J. Lett. 187 (1974) L101.
2. W. Hillebrandt, F.K. Thielemann, Ap. J. 255 (1982) 617.
3. M. Wiescher, K. Langanke, Z. Phys. A325 (1986) 305.

4. R.K. Wallace, S.E. Woosley, Ap. J. Suppl. 45 (1981) 389.
5. R.E. Taam, Ann. Rev. Nucl. Part. Sci. 35 (1985) 1.
6. M. Wiescher, J. Görres, F.K. Thielemann, H. Ritter, Astron. Astrophys. 160 (1986) 56.
7. P.M. Endt, C. van der Leun, Nucl. Phys. A310 (1978) 1.
8. B. Sherrill, PhD Thesis, Hadr. J. Suppl. to be published.
9. W. Benenson, A. Guichard, E. Kashy, D. Mueller, H. Nann, L.W. Robinson, Phys. Lett. B58 (1975) 46.
10. W. Benenson, E. Kashy, Rev. Mod. Phys. 51 (1979) 527.
11. W.E. Ormand, B.A. Brown, Nucl. Phys. A to be submitted.
12. B.A. Brown, B.H. Wildenthal, Nucl. Data. Tabl. 33 (1985) 347.
13. W.A. Fowler, G.R. Caughlan, B.A. Zimmerman Ann. Rev. Astr. Ap. 13 (1975) 69.
14. C. Rolfs, Nucl. Phys. A217 (1973) 29.
15. Wiescher, et al., Nuclear Physics A (In Press).

STUDIES OF T = 1/2 LEVELS IN  ${}^9\text{Be}$  AND  ${}^9\text{B}$  WITH THE  ${}^6\text{Li}({}^6\text{Li}, {}^3\text{He}){}^9\text{Be}$  AND  ${}^6\text{Li}({}^6\text{Li}, t){}^9\text{B}$  MIRROR REACTIONS, AND WITH THE  ${}^{11}\text{B}(p, t){}^9\text{B}$  REACTION

D. Mikolas, W. Benenson, B.A. Brown, Y. Chen, E. Kashy, J.A. Nolen Jr., P. Rutt, B. Sherrill, J.S. Winfield, R. Harkewicz, R. Sherr<sup>a</sup>, J.D. Brown<sup>a</sup>, and R. Kouzes<sup>a</sup>

Low Lying Levels from  ${}^6\text{Li}({}^6\text{Li}, {}^3\text{He}){}^9\text{Be}$  and  ${}^6\text{Li}({}^6\text{Li}, t){}^9\text{B}$

We have previously reported the first measurement of the beta-decay branching-ratios of  ${}^9\text{C}$  to the first three negative parity levels in  ${}^9\text{B}^{1,2,3}$  ( $3/2^-$ ; g.s.,  $5/2^-$ ; 2.36 MeV, and  $1/2^-$ ; 2.9 MeV). A level at 12 MeV was also populated, with a B(GT) of at least 1.5.<sup>3</sup> This level can not be directly associated with any of those reported in the Ajzenberg-Selove<sup>4</sup> compilations. The beta decay of  ${}^9\text{Li}$  is known to strongly populate a level in  ${}^9\text{Be}$  which is also near 12 MeV (see discussion in Ref. 3). We therefore have attempted to observe this level, and its analog in  ${}^9\text{Be}$  with the  ${}^6\text{Li}({}^6\text{Li}, t){}^9\text{B}$  and  ${}^6\text{Li}({}^6\text{Li}, {}^3\text{He}){}^9\text{Be}$  mirror reactions. This level is predicted by the shell model to have a strong spectroscopic factor for this reaction.

We had originally planned to use a simple arrangement of silicon detector telescopes to simultaneously detect the outgoing  ${}^3\text{He}$ 's and t's in order to directly compare the level structure and shift at each angle. However, the large kinematic shift associated with comparable-mass particles limited the useful solid angle of the detectors. Instead, we used the S320 spectrograph with both of its position sensitive wires active to correct for scattering angle within the acceptance. A beam energy of 66 MeV was chosen as a compromise. This was the highest energy available at the time for the  ${}^6\text{Li}^{+1}$  ion due to high-voltage limits within the cyclotron. At the lowest available energy for the  ${}^6\text{Li}^{+2}$  ion, the rigidity of the outgoing triton would have been above K=320 for the ground state of  ${}^9\text{B}$ , and thus would have been impossible to observe.

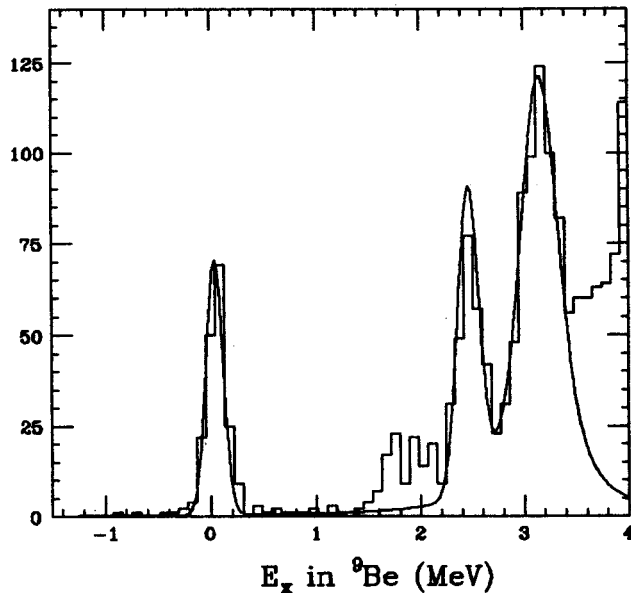


Fig. 1: Excitation energy in  ${}^9\text{Be}$  from the reaction  ${}^6\text{Li}({}^6\text{Li}, {}^3\text{He})$  at  $E = 66$  MeV and a scattering angle of  $3^\circ$  in the lab. The smooth curve is a fit described in the text.

Targets of enriched  ${}^6\text{Li}$  and  ${}^7\text{Li}$  were evaporated on to thin Formvar films (containing C, H and O) to a thickness of approximately  $200 \mu\text{g}/\text{cm}^2$  each. Lithium can not easily be rolled to a thickness below a few  $\text{mg}/\text{cm}^2$ .<sup>5</sup> The thickness of the Formvar was not determined. The solvent was repeatedly diluted until the films became impossible to produce without holes. These were somewhat thinner than films which produced color from the onset of interference of reflected visible light. A thick, bare Formvar target was also included in the target load of the spectrograph to help identify the Oxygen and Carbon lines.

Carbon films were not used for a backing material, even though they can be obtained much thinner than Formvar can be produced. The evaporation of Lithium is not compatible with

thin Carbon foils. They buckle and fold as soon as the evaporation begins.<sup>6</sup> The melting point of Lithium is low, thus this is not likely to simply be a thermal effect. Instead, some sort of chemical interaction is suspected. If this is the case, the evaporation of a thin barrier layer of some other material may allow for the use of carbon backings with Lithium. Alternatively, perhaps thin gold foils could be used.

Extensive data were taken at 3° (lab) for the  $^3\text{He}$ 's (levels in  $^9\text{Be}$ ), and at 3° and 7° for the tritons (levels in  $^9\text{B}$ ). The data above 4 MeV excitation energy in both nuclei were contaminated with many lines from Carbon and Oxygen, and are presently being analyzed for narrow lines from Mass 9.

Figure 1 shows the low excitation energy spectrum for  $^9\text{Be}$ . The ground state and the narrow  $5/2^-$  state at 2.43 MeV serve as an internal excitation energy calibration. The smooth line represents a fit to the data. The width of the ground state peak is used to define the instrumental resolution. The location and width of the  $5/2^+$  state are taken from Ref. 4. Its shape is that of a gaussian which represents the instrumental resolution, folded with a Lorentian with the appropriate width. The amplitudes have been adjusted to match the areas of the peaks. The fit is quite good.

To study the analogous region in  $^9\text{B}$  (Fig. 2), the ground state was fit in a similar way to that of the ground state of  $^9\text{Be}$ . The ratios of  $5/2^-$  to ground state, and of  $5/2^+$  to ground state areas were fixed to those ratios in  $^9\text{Be}$ . The centroid and width of the  $5/2^-$  and  $5/2^+$  levels have again been taken from Ref. 4. While the fit to the ground state and  $5/2^-$  level is good, there seems to be a problem with the fit to the  $5/2^+$  level. It is not clear at present what could cause such a disagreement. Two effects are under consideration. The first is that there is some strength to the broad  $1/2^-$  state at 2.9 MeV in both nuclei, and that it has

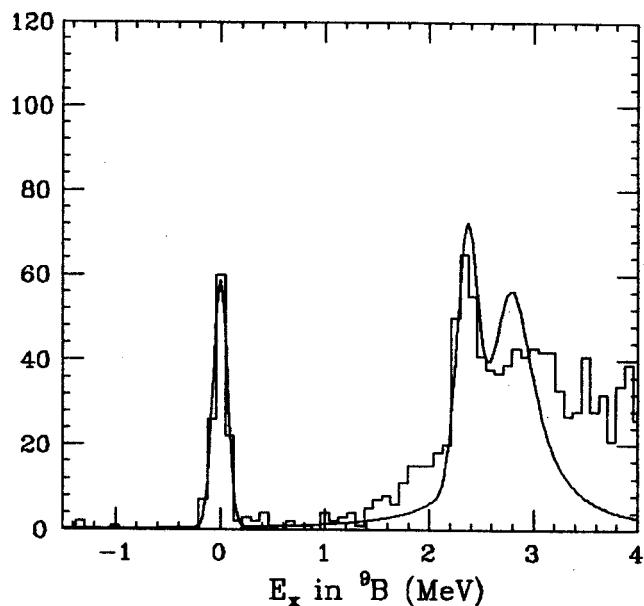


Fig. 2: Excitation energy in  $^9\text{B}$  from the reaction  $^6\text{Li}(^6\text{Li},t)$ , using the same target, beam energy, and scattering angle as the data in fig. 1. The smooth curve is described in the text.

not been properly subtracted from the data. While the dip between the  $5/2^-$  and  $5/2^+$  levels in the spectra might be the best indicator of the weakness of the  $1/2^-$  state, its exact shape is not clear (see Ref. 3 and references therein). A spectrum with higher statistics, and perhaps better resolution would be useful.

The second effect has to do with the reaction itself. It has been reported that below a certain energy, the outgoing particle wave-function is so distorted that accurate spectroscopic factors may not be determined, and that excitation energy spectra may become distorted.<sup>7</sup> Any attempt to understand the spectrum within the framework of this phenomenon will require both a survey of other mirror reactions and the study of the behavior of the 0-4 MeV region as the beam energy is varied below and above 66 MeV.

If indeed the second effect is important, then the data near 12 MeV will be even more distorted, since the outgoing  $A = 3$  particle will have even lower energy.

The most intriguing feature of these spectra is the possible presence of the  $1/2^+$  first excited states of  ${}^9\text{Be}$  and  ${}^9\text{B}$ . The level has been well characterized in  ${}^9\text{Be}$ , and studied in  ${}^9\text{B}^{8-12}$ , and lies just above the neutron threshold in  ${}^9\text{Be}$  at 1.665 MeV. It has an asymmetrical shape, and the folding of this shape with the instrumental resolution could easily explain the 'bump' in  ${}^9\text{Be}$  between 1.7 and 2.2 MeV. However, this bump could also be explained by the tail of the  $1/2^-$  level if it is indeed present. The shift of this bump in  ${}^9\text{B}$  might be explained as the increase of the barrier of the  $l = 1$  nucleon from centrifugal to centrifugal+Coulomb as the nucleon is changed from a neutron to a proton. However, the nucleon decay threshold drops from 1.665 MeV in  ${}^9\text{Be}$  to -0.185 MeV in  ${}^9\text{B}$ , which could offset this effect. Further study is clearly needed to understand the exact shapes of the  $1/2^-$  and  $5/2^+$  levels in both  ${}^9\text{Be}$  and  ${}^9\text{B}$ .

Candidates for a  $T = 1/2$ , Isospin Mixing Level in  ${}^9\text{B}$  with the  ${}^{11}\text{B}(p,t){}^9\text{B}$  reaction

The lowest  $A = 9$   $T = 3/2$  quartet is the only quartet known to demonstrate significant deviation from the quadratic Isobaric Mass Multiplet Equation.<sup>13-15</sup> The IMME is an expression for the masses of an isospin multiplet as a function of  $T_z$ ;

$$\text{Mass} = a + bT_z + cT_z^2 + dT_z^3 + \dots$$

The masses of the ground states of  ${}^9\text{C}$  and  ${}^9\text{Li}$ , and the first  $T=3/2$  levels in  ${}^9\text{B}$  and  ${}^9\text{Be}$  give a value for  $d$  of  $7.6 \pm 1.7$  keV when all higher terms are set to zero.<sup>13</sup> An isospin-conserving hamiltonian results in a strictly quadratic form of the IMME. Therefore, one explanation for this deviation could be isospin mixing of the  $J^\pi = 3/2^-, T = 3/2$  levels in  ${}^9\text{Be}$  and  ${}^9\text{B}$  with nearby  $T = 1/2$  levels of the same spin and parity. In order to account for the masses of all four nuclei, the shift of the levels in  ${}^9\text{Be}$  and  ${}^9\text{B}$  should both be downward, which would indicate

the presence of a level roughly one or two MeV above the analog states in both nuclei. These levels should have a width much less than 100 keV to account simultaneously for the observed widths and calculated shifts of these levels.

A search for the proposed level, similar to that of Hardy et al.<sup>16</sup>, was carried out with the  ${}^{11}\text{B}(p,t){}^9\text{B}$  reaction. A beam of 42 MeV protons was accelerated by the K-50 cyclotron at Princeton University. The QDDD spectrograph was used with a solid angle of 14 msr to observe the outgoing tritons. If a level were to be found, the angular distribution from this reaction could be used to indicate if the spin and parity are  $3/2^-$ . No narrow candidates were observed for a new level that could be mixed with the  $T = 3/2$  level. However, a possible level at 15.2 MeV with a width of roughly 150 keV was observed (see Fig. 3). While the parameters of this level are not certain (the continuum is quite

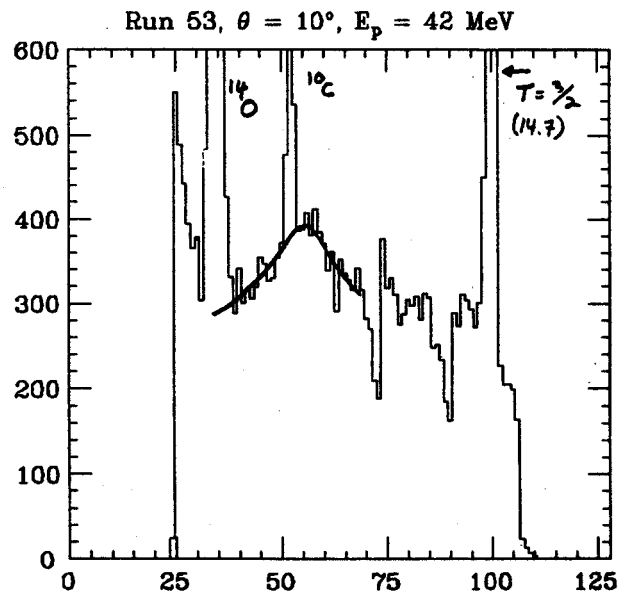


Fig. 3: Position spectra taken with the Princeton QDDD spectrograph, from the reaction  ${}^{11}\text{B}(p,t){}^9\text{B}$ . The energy of the proton beam was 42 MeV. Contaminant lines from Oxygen and Carbon are strong but well separated. The proposed 15.2 MeV level has a width between 100 and 200 keV. A solid line has been drawn to guide the eye. Dips in the spectrum near channels 75 and 90 are the result of bad charge collection coupled with a narrow PID gate.

strong under this bump), it is consistent with a level reported by Hardy et al.<sup>16</sup> Excitation energies up to 18 MeV were observed. No other interesting features have yet been detected in the data, which are presently under analysis.

a. Princeton University, Princeton, NJ.

#### References

1. J. Stevenson, J.A. Nolen Jr., D. Mikolas, W. Benenson, L.H. Harwood, E. Kashy, R. Sherr, B. Sherrill, Z.Q. Xie and J.S. Winfield, NSCL Ann. Rep., (1985), 91.
2. D. Mikolas, B.A. Brown, W. Benenson, Y. Chen, M.S. Curtin, L.H. Harwood, E. Kashy, J.A. Nolen Jr., M. Samuel, B. Sherrill, J. Stevenson, A. Vander Molen, J.S. Winfield, Z.Q. Xie, R. Sherr, M. Gai, Z. Zhao, Proceedings of the 5th International Conference on Nuclei Far From Stability, Rosseau Lake., I. Towner, Ed., AIP, NY (1988).
3. D. Mikolas, B.A. Brown, W. Benenson, L.H. Harwood, E. Kashy, J.A. Nolen Jr., B. Sherrill, J. Stevenson, J.S. Winfield and Z.Q. Xie, Phys. Rev. C37, (1988), 766.
4. F. Ajzenberg-Selove, Nucl. Phys. A413, (1984), 1.
5. S. Austin, NSCL, Private Communication.
6. Zeb Ayer; Notre Dame, Private Communication.
7. S.W. Cosper, H. Brunnader, J. Cerny and L. McGrath, Phys. Lett. B25, (1967), 324.
8. R.R. Spencer, G.C. Phillips and T.E. Young, Nucl. Phys. 21, (1960), 310.
9. R. Sherr and G. Bertsch, Phys. Rev. C32, (1985), 1809.
10. F. Barker, Australian J. Phys., 40, (1987), 307.
11. G. Kuechler, A. Richter and W. von Witsch, Z. Phys. 326, (1987), 447.
12. K. Kadija, G. Paic and B. Antolkovic, Phys. Rev. C36, (1987), 1269.
13. E. Kashy, W. Benenson and J.A. Nolen Jr., Phys. Rev. C9, (1974), 2102.
14. N. Auerbach, A. Lev and E. Kashy, Phys. Lett. B36, (1971), 453.
15. W. Benenson and E. Kashy, Rev. Mod. Phys., 51, (1979), 527.
16. J.C. Hardy, J.M. Loiseaux, J. Cerny and G. T. Garvey, Nucl. Phys. A162, (1971), 552.



U. Garg<sup>a</sup>, A. Braun<sup>a,b</sup>, K.B. Beard<sup>a</sup>, A. Galonsky, Y.-W. Lui<sup>c</sup>, T. Murakami, J.S. Winfield, D. Ye<sup>a</sup>, and D.H. Youngblood<sup>c</sup>

We have employed a 700 MeV  $^{14}\text{N}$  beam (50 MeV/nucleon) to excite giant resonances (GR) in  $^{58}\text{Ni}$ ,  $^{64}\text{Ni}$ ,  $^{90}\text{Zr}$ ,  $^{116}\text{Sn}$ ,  $^{144}\text{Sm}$ , and  $^{154}\text{Sm}$ . The basic aim of these studies has been to investigate the High Energy Octupole Resonance (HEOR) and, in conjunction with our earlier data at  $E/A=35\text{ MeV}^1$  and  $40\text{ MeV}^2$ , to attempt to understand the continuum contributions at excitation energies above 15 MeV or so.

At low projectile energies ( $E/A \leq 25\text{ MeV}$ ), the angular distributions from heavy-ion (HI) inelastic scattering are dominated by Coulomb effects and are essentially featureless, peaking at the grazing angles. At the higher energies ( $E/A > 35\text{ MeV/A}$ ), at least for lighter projectiles and targets, nuclear and surface effects are expected to begin to dominate, leading to diffractive angular distributions characteristic of the angular momentum transfer,  $\ell$ . In addition, as angular momentum matching conditions improve at higher energies, stronger excitation of higher- $\ell$  resonances would be expected. This is borne out by CCBA calculations (shown in Fig. 1) which indicate that the peak cross-section for the HEOR, for example, increases by almost two orders of magnitude between 20 MeV/nucleon (typical of previous HI studies) and 50 MeV/nucleon (now available at NSCL for  $^{14}\text{N}$  beams). Further, as shown in the figure, the HEOR excitation with  $^{14}\text{N}$  is predicted to be more than an order of magnitude larger than that with 43 MeV/nucleon  $\alpha$  particles and even better than the GQR cross section for  $\alpha$  particles of comparable energies; at the same time it is hoped that the heavy-ion spectra would have lower continuum contributions.

The predicted angular distributions for the excitation of  $\ell=0, 2$  and  $3$  modes at energies

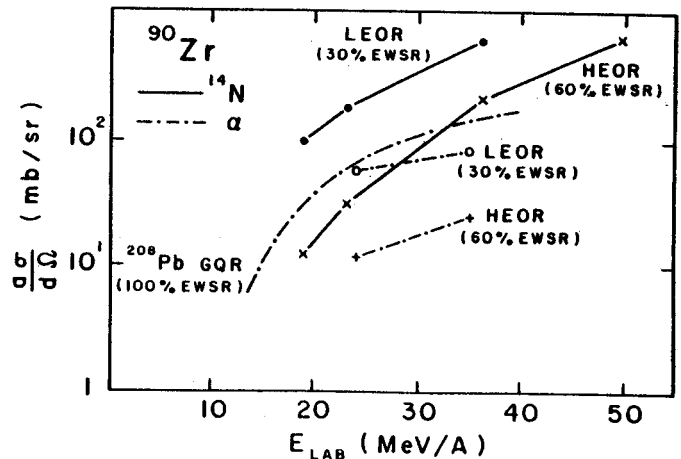


Fig. 1: CCBA predictions of the peak cross-sections for the excitation of LEOR and HEOR in  $^{90}\text{Zr}$  with  $^{14}\text{N}$  projectiles as a function of the bombarding energy (solid lines). DWBA calculations for excitation of indicated giant resonances with alpha particles (dash-dot lines) are also shown.

corresponding to the known positions of the GMR, GQR, and HEOR, respectively, using  $^{14}\text{N}$  projectiles at 50 MeV/nucleon are shown in Fig. 2. These have diffraction-like structure characteristic of the  $\ell$ -value and it is clear that, in the range of our measurements ( $3^\circ$  to  $7^\circ$ ), it should be possible to distinguish between different multipolarities, adding a very important tool hitherto absent in heavy ion scattering measurements. For these calculations, as well for those shown in Fig. 1, the code ECIS<sup>3</sup> was used with appropriate form factors; similar results were obtained independently from another code PTOLEMY<sup>4</sup>.

$^{14}\text{N}$  beams at these energies afford several distinct advantages over other projectiles in this mass range for these studies. There are no strongly excited projectile states (such as the 6.1 MeV group in  $^{16}\text{O}$ ) that would interfere seriously with the GR region; at these energies,

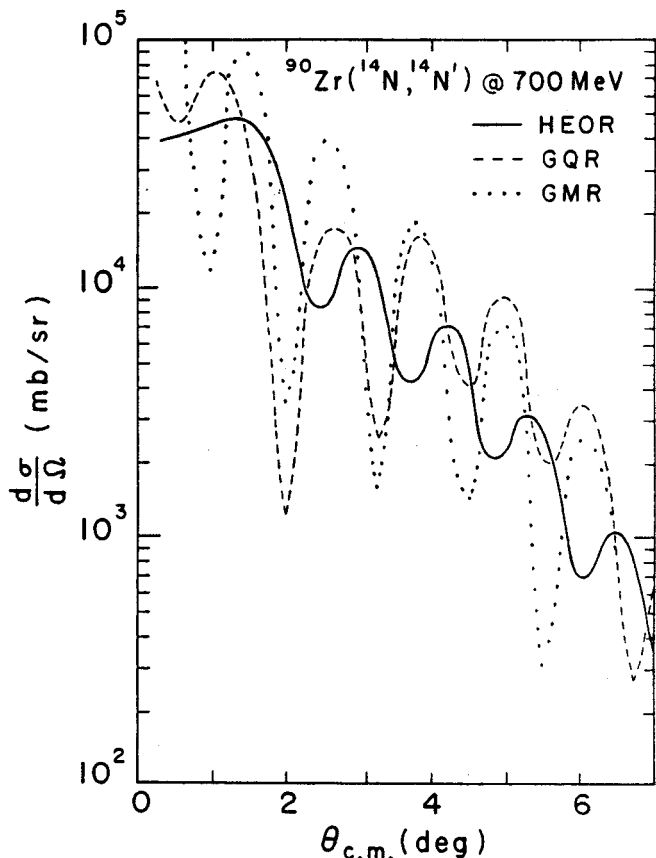


Fig. 2: CCBA predictions for angular distributions for the excitation, by 700 MeV  $^{14}\text{N}$  projectiles, of  $\ell=0, 2, 3$  modes in  $^{90}\text{Zr}$  at energies corresponding to the known positions of the GMR, GQR, and HEOR, respectively. For exhaustion of 100% of the EWSR, these cross-sections must be multiplied by the appropriate  $\beta^2$ .

the interfering "pick-up and decay" reactions<sup>5</sup> lie well above 40 MeV in excitation and, hence, are not a problem; and, with the new ECR source, abundant beams of 50 MeV/nucleon  $^{14}\text{N}$  beams are now available at NSCL.

Inelastically scattered  $^{14}\text{N}$  ions were detected in the focal plane of the S320 spectrograph; the detector system consisted of two single-wire proportional counters, two ionization chambers, and a scintillator. This arrangement not only provided good charge and mass separation for the reaction products but also, and perhaps, equally important for this type of study, permitted ray-tracing and angle-

reconstruction. This combined with an active collimator system, ensured final spectra that were virtually free of all non-physical contributions. The angular bite of the spectrograph was about  $1.2^\circ$ . The angle-reconstruction technique allowed each run to be broken into three angles each of  $.25^\circ$  width with a smaller cut at each side for normalization with the data at adjacent angles. There was still sufficient opening to fully avoid the edges of the slit. A rather complete set of angular distributions (up to 15 angles between  $3^\circ$  and  $7^\circ$ , allowing for more than two complete oscillations in the angular distributions for  $\ell=3$  transfer) were obtained for  $^{90}\text{Zr}$  and  $^{116}\text{Sn}$ ; for the other targets, data were obtained only for one angular bite. In addition, elastic scattering data were taken for  $^{90}\text{Zr}$  and  $^{208}\text{Pb}$  between  $1.75^\circ$  and  $7^\circ$  to obtain absolute normalizations. For energy calibration purposes, data were also obtained at all angles with a  $^{12}\text{C}$  target. Here we report preliminary results on  $^{116}\text{Sn}$  and results of an experimental test of a newly proposed relationship between the energy and width of the GQR and the neutron binding energy ( $S_n$ ) of the target nucleus.

Sample spectra for  $^{116}\text{Sn}$  are presented in Fig. 3 for two angular bites. Within each set, no further relative normalization is required since the data were taken at the same time, and the angle-width chosen for each angle is the same ( $.25^\circ$ ). A very conservative estimate of the background is also indicated and the expected location of the HEOR is shown by arrows. It is clear from these spectra that there is significant strength in the HEOR region and, further, that this strength does show an angular dependence; this angular dependence, on further analysis, appears to be consistent with the expected angular distribution for the  $\ell=3$  mode. A detailed analysis of the data to extract the relevant GR parameters is still in progress but the positions and widths of the resonances are consistent with previously reported values<sup>6</sup>.

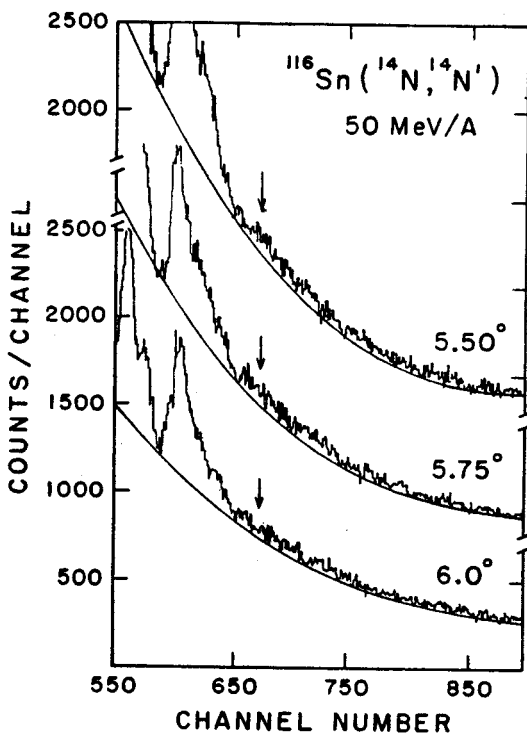
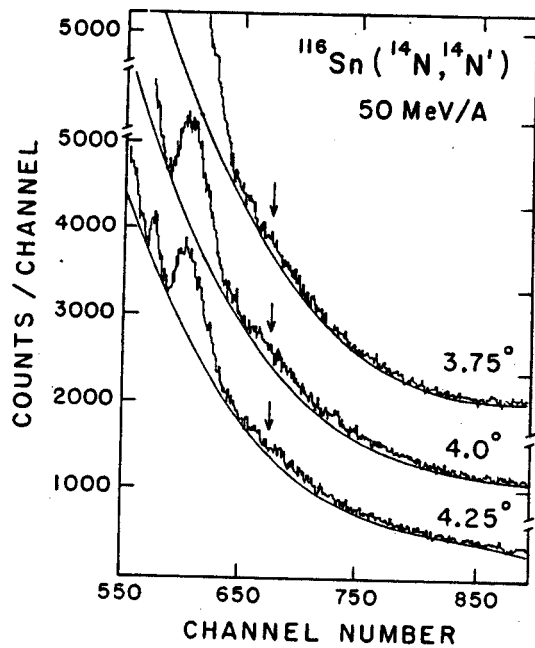


Fig. 3: a) Sample spectra for  $^{116}\text{Sn}$  for the angular bite centered at  $4.0^\circ$ . The solid lines represent assumed shapes of the continuum (subtracted from the spectra for further analysis). The approximate position of the HEOR is indicated. All three spectra were taken in one run and the three angles reconstructed by ray tracing. b) Same as (a) but for the angular bite centered at  $5.75^\circ$ .

Other features apparent in these spectra are:

i) there is a very strong excitation of the GMR+GDR+QGR bump, consistent with other HI measurements;

ii) there are no high-lying structures similar to those reported in Ref. 7;

iii) no significant contributions are observed from the "pick-up and decay" channels even up to more than 40 MeV excitation energy; and

iv) the continuum in the region of the HEOR obscures its observation. The last feature is somewhat surprising since, in general, HI scattering is expected to produce lower backgrounds. As a result of the high continuum contributions, the HEOR does not "stand out" in the spectra as dramatically as we had hoped it would. Indeed, the nature of this continuum itself would make a very interesting study, and we plan to try to understand it using these data in conjunction with our earlier data at 35 and 40 MeV/nucleon.

We turn our attention now to a new relationship recently proposed by Loveman and Peterson<sup>8</sup> between the centroid and width of the GQR and the  $S_n$  of the nucleus. The excitation energy of the GQR has been known to follow a dependence on the mass of the nucleus given by the expression  $E_x = 64 A^{-1/3} \text{ MeV}^{12}$ . A less rigorous relationship between the width of the GQR and the mass has also been widely accepted, viz.,  $\Gamma = 90 A^{-2/3} \text{ MeV}^9$ . Loveman and Peterson (LP), however, have suggested a new relationship between the excitation energy and width of the GQR, and the neutron separation energy of the excited nucleus. With very few exceptions, these quantities should follow a rather simple relationship,

$$E_x = S_n + C \times \Gamma,$$

where the constant  $C = 0.91$  was determined from fits of this expression to the known data. The

quality of this fit, as determined by the  $\chi^2$  values, is similar to the fits to the aforementioned expression for the mass dependence of the excitation energy of the GQR.

An easy way to test the validity of this relationship is to compare the GQR parameters of two or more isotopes which differ significantly in their  $S_n$  values. The nuclei  $^{58}\text{Ni}$  and  $^{64}\text{Ni}$  provide an excellent, and rather convenient, test case--their neutron binding energies differ by 2.54 MeV<sup>10</sup> and the GQR region is free from a strong excitation of the GMR<sup>11</sup>, making the extraction of the GQR parameters less complicated.

For the specific purpose of testing the validity of the LP expression, we made measurements for  $^{58}\text{Ni}$  and  $^{64}\text{Ni}$  sequentially without changing the experimental conditions between the runs. The targets consisted of isotopically enriched (>98%) self-supporting foils of nearly equal thickness (each approximately 2mg/cm<sup>2</sup>). Data were also taken with a  $^{12}\text{C}$  target for energy calibration purposes.

Samples of spectra for the two nuclei are shown in Fig. 4. There is no discernible difference between the GR "bumps" in the two cases; this holds true for data at three different angles. Peak-fit analyses of the data confirm that the centroid and width of the GQR differ at most by a few hundred keV, in tune with the previously established relationship but in sharp contrast with the predictions of LP--according to the LP relationship, either the centroid of GQR in  $^{64}\text{Ni}$  would have to be lower by as much as 2.54 MeV, or the width would have to increase by 2.8 MeV (or some combination of the two effects). Thus, our results indicate that, the LP relationship is clearly ruled out for these nuclei.

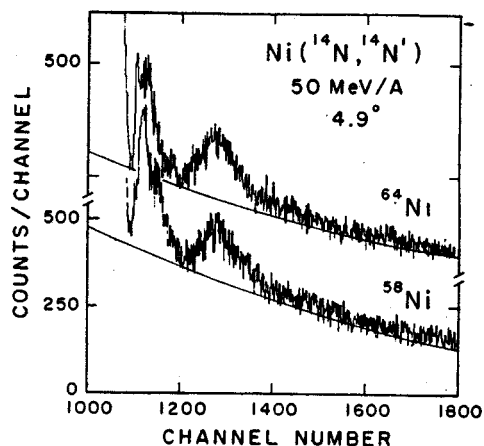


Fig. 4: Spectra for  $^{58}\text{Ni}$  and  $^{64}\text{Ni}$  at  $4.9^\circ$ ; the possible shapes for the continuum are indicated by solid lines. The main resonance "bump" consists primarily of the GQR with some possible contribution from the GDR on the higher excitation energy side.

- a. Univ. of Notre Dame, Notre Dame, Indiana.
- b. REU student from St. Norbert's College, De Pere, Wisconsin.
- c. Texas A&M Univ., College Station, Texas.

#### References

1. U. Garg et al., J. Phys. Soc. Jpn. 54 Suppl. II, 505 (1985).
2. U. Garg et al., Bull. Am. Phys. Soc. 31, 1205 (1986).
3. Obtained from J. Raynal, CEN, Saclay; J. Raynal, Phys. Rev. C23, 2571 (1981).
4. M.J. Rhoades-Brown, S.C. Pieper, and M.H. Macfarlane, Phys. Rev. C21, 2417 (1980).
5. C. Gelbke, in Giant Resonances, edited by F.E. Bertrand (Harwood, New York, 1980)pp. 333.
6. T.A. Carey et al., Phys. Rev. Lett. 45, 239 (1980); H.P. Morsch et al., Phys. Rev. Lett. 45, 337 (1980); T. Yamagata et al., Phys. Rev. C23, 937 (1981).
7. Ph. Chomaz et al., Z. Phys. A319, 41 (1984); N. Frascaria et al., Nucl. Phys. A474, 253 (1987).
8. R.A. Loveman and R.J. Peterson, Z. Phys. A328, 281 (1987).
9. See, for example, F.E. Bertrand, Nucl. Phys. A354, 129c (1981).
10. A. Wapstra and K. Bos, Atomic Data and Nuclear Data Tables 19, 215 (1977).
11. U. Garg et al., Phys. Rev. C25, 3204 (1982), and references therein.

THE  $^{208}\text{Pb}(^7\text{Li}, ^6\text{Li}), (^7\text{Li}, ^6\text{He})$  REACTIONS AT  $E(^7\text{Li}) = 140$  MeV AND THE SINGLE PARTICLE LEVELS AND STABILITY OF HEAVY NUCLEI ( $A > 200$ ).

F.D. Becchetti,<sup>a</sup> D.A. Roberts,<sup>a</sup> J.W. Janecke,<sup>a</sup> A. Nadasen,<sup>b</sup> C.A. Ogilvie and J.S. Winfield.

The existence of an island of nuclear stability near  $Z = 114$  or  $126$  and with  $A = 300$  to  $360$  has long been predicted. Experimental verification of semi-stable, super heavy nuclei (SHE) has been the focus of several H.I. accelerator research programs. The GSI group<sup>1</sup>, in particular, has found evidence of increased  $\alpha$ -stability as  $Z \rightarrow 110$ .

The atomic number, masses and stability of heavy nuclei, in particular superheavy elements (SHE's) with  $A \approx 300$ , are determined primarily by the ordering and energies of the proton and neutron single-particle (s.p.) levels. In particular, the location of high- $j$  levels ( $1j_{13/2}$ ,  $1k_{17/2}$ , ...) are critical to the determination of the  $Z$  and  $N$  (and mass) of the SHE's. Most predictions for the latter are based on extrapolation of the low- $j$  s.p. levels ( $A \leq 210$ ). This may not be reliable as there appear to be  $j$ -dependent effects (beyond the usual spin-orbit force) in nuclear s.p. potentials. Extrapolations to  $A \approx 300$  seldom agree on the exact sequence and energy-spacing of s.p. levels. Additional experimental data on high- $j$  s.p. levels in nuclei around  $A \approx 200$  should provide a better basis for extrapolating s.p. levels to  $A = 300$ . Previously, we and others have studied the  $(^{16}\text{O}, ^{15}\text{O})$  (Ref. 2) and  $(^{12}\text{C}, ^{11}\text{C})$  reactions as well as  $(\alpha, ^3\text{He})$  (Ref. 3) and  $(\alpha, t)$  in order to excite preferentially high- $j$  s.p. levels. Also, a  $j$ -dependence in the small angle cross section, arising from the  $j$ -dependence of the heavy-ion transfer selection rules, has been observed. This can be used to distinguish  $j_>$  from  $j_<$  states. The  $j_>$  states are complicated by excited ejectile states, whereas the  $j_<$  states are limited in their momentum transfer.

For these reasons we have initiated a study of the  $^{208}\text{Pb}(^7\text{Li}, ^6\text{Li})^{209}\text{Pb}$  and  $^{208}\text{Pb}(^7\text{Li}, ^6\text{He})^{209}\text{Bi}$  reactions at  $E(^7\text{Li}) = 140$  MeV. Although these reactions have been studied<sup>4</sup> at lower energies, a higher  $^7\text{Li}$  energy is needed to excite high- $j$  levels. The present data were obtained with a  $350 \mu\text{g}/\text{cm}^2$   $^{208}\text{Pb}$  target and the reaction products were detected by the S-320 spectrometer. Sample spectra are shown in Figs. 1 and 2. Analysis of the data is in progress, including finite-range DWBA for the extraction of  $S_n$  and  $S_p$  values. Since the high- $j$  strength appears to be fragmented, the latter will be required to deduce the high- $j$  s.p. centroids.

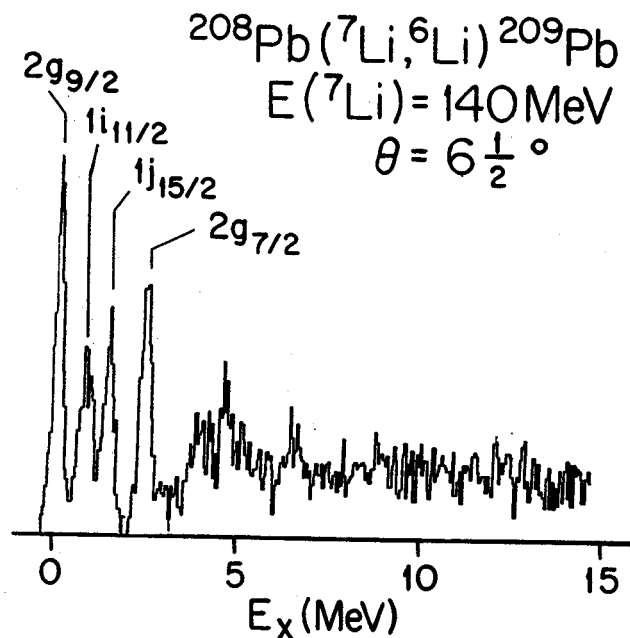


Fig. 1 Spectrum of the  $^{208}\text{Pb}(^7\text{Li}, ^6\text{Li})^{209}\text{Pb}$  reaction at 140 MeV. Low lying s.p. states are indicated.

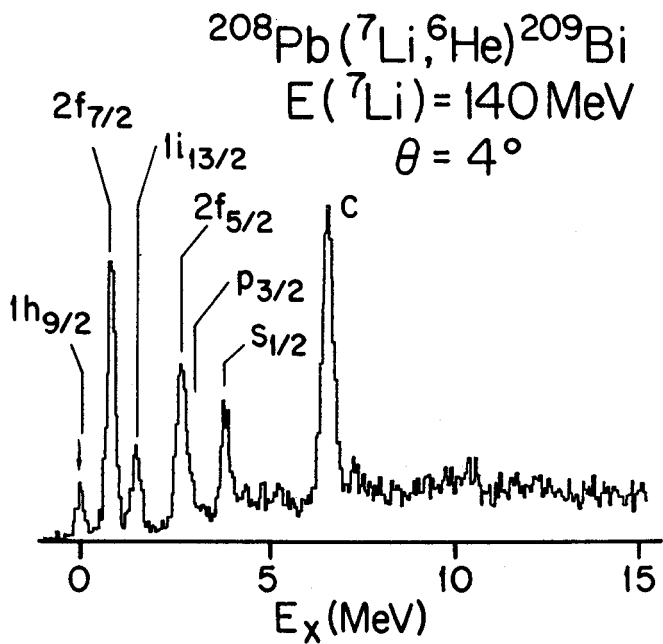


Fig. 2 Spectrum of the  $^{208}\text{Pb}(^7\text{Li}, ^6\text{He})^{209}\text{Bi}$  reaction at 140 MeV. Low lying s.p. states are indicated.

- a. University of Michigan, Ann Arbor, MI.
- b. University of Michigan, Dearborn, MI.

#### References

1. P. Armbruster et al., Z. Phys. A324, 489 (1986).
2. F.D. Becchetti et al., Phys. Rev. C 12, 894 (1975).
3. C.P. Massolo et al., Phys. Rev. C 34, 1256 (1986).
4. A.F. Zeller et al., Nucl. Phys. A332, 515 (1979).

Z. Zhao,<sup>a</sup> M. Gai,<sup>a</sup> B.J. Lund,<sup>a</sup> S.M. Rugari,<sup>a</sup> D. Mikolas, B.A. Brown, J.A. Nolen Jr., M. Samuel

We have studied the beta-delayed alpha emission of  $^{18}\text{N}$  in preparation to a proposed parity-violation experiment, the alpha decay of the  $0^-$  state at 6.88 Mev in  $^{18}\text{O}$ . In the present work,  $^{18}\text{N}$  was produced by the fragmentation of a 35 MeV/u  $^{22}\text{Ne}$  beam from the MSU K500 cyclotron, by a thick Ta target. The  $^{18}\text{N}$  ions were separated from other reaction products and the beam by the MSU Reaction Product Mass Separator (RPMS). The detector system was situated at the focal plane of the RPMS; it consists of a two-dimensional position-sensitive gas counter and five thin surface barrier detectors tilted 45° to the RPMS axis, in order to minimize the energy loss from beta rays. The vertical position signal of the gas counter is proportional to the m/q of the detected particles. A particle identifier (PID), defined as  $(E+dE)^{1.78} - E^{1.78}$ , allowed us to identify the nuclei at the focal point. During the beam-on period,  $^{18}\text{N}$  nuclei were implanted into the detectors, and the number of nuclei stopped inside the detectors was measured. Alpha-particle spectra were recorded during the beam-off cycle of approximately 1 second. The efficiency for alpha detection was calculated from the known lifetime.

Table 1 gives our measured branching ratios and log ft values of the beta decay of  $^{18}\text{N}$  to the  $1^-_3$  and  $1^-_4$  states in  $^{18}\text{O}$  assuming a 100% alpha branch. Various theoretical predictions are listed in the same table. In figure 1(a) we show the E1 vs E2 spectrum, where E1 and E2 are two adjacent silicon detectors. In fig 1(b) we show the same data with a veto on nuclei punching through detector number 2 (E2) produced by detector number three (E3). In figure 2 we show the beta delayed alpha-particle spectrum of  $^{18}\text{N}$ , showing the alpha lines corresponding to the decay of the  $1^-_3$  and  $1^-_4$  states and an

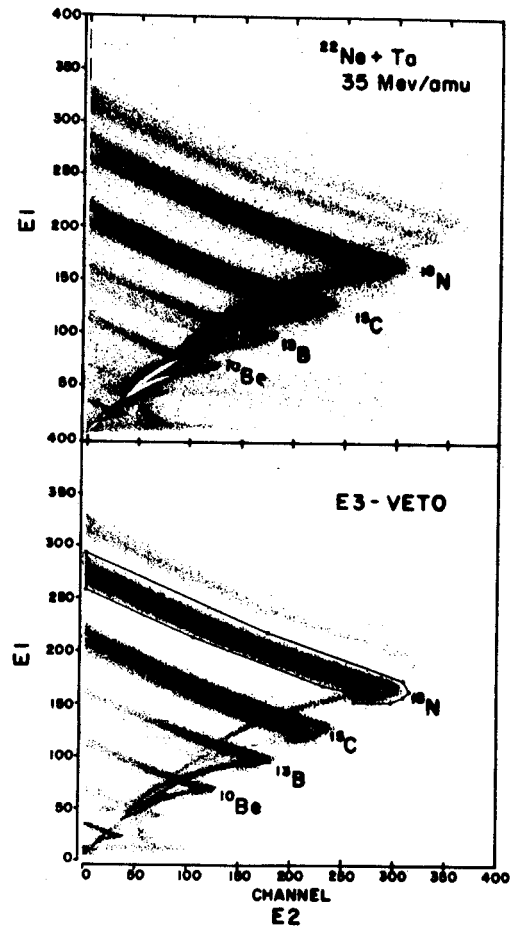


Fig. 1: Reaction products from 35 MeV/u  $^{22}\text{Ne}$  beam on Ta target.

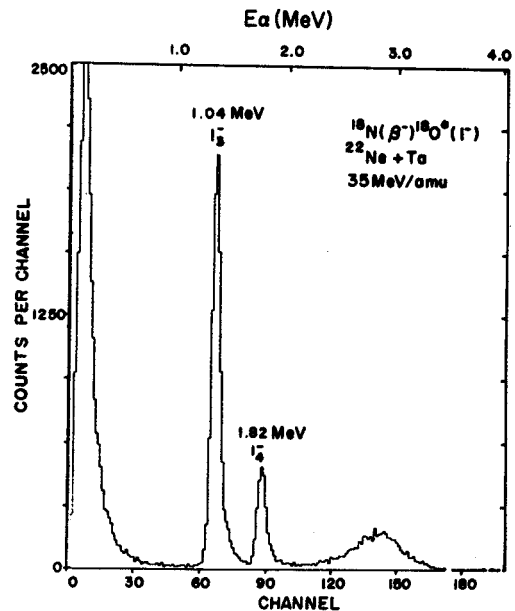


Fig. 2: Beta delayed alphas emitted from  $^{18}\text{N}$ .

unresolved group of states around 9.00 MeV excitation energy in  $^{18}\text{O}$ .

We plan to study the parity nonconserving alpha decay of the  $0^-$  state of  $^{18}\text{O}$  at 6.88 MeV<sup>1</sup>. This  $0^-$  state will be populated by the beta decay of  $^{18}\text{N}$  (branching ratio 15%) produced in a nuclear reaction, using the upgraded ESTU-Yale tandem. The proposed experiment is similar to the study of the  $2^-$  state in  $^{16}\text{O}$  populated in the beta decay of  $^{16}\text{N}$ <sup>3</sup>, but the  $1^-$  state in  $^{18}\text{O}$  is considerably narrower than the one in  $^{16}\text{O}$ . The measured absolute beta decay branching ratio of  $^{18}\text{N}$  to  $1^-_3$  and  $1^-_4$  states in  $^{18}\text{O}$  will provide normalization for the parity experiment. In the proposed experiment, we plan to reduce the background by several orders of magnitude by the use of beta-alpha coincidence and time of flight measurement. The present study of the beta decay of  $^{18}\text{N}$  allows us to understand the background to the future parity violation experiment.

Supported in part by U.S. Department of Energy Contract No. DE-AC02-76ER03074 and the NSF.

a. A.W. Wright Nuclear Structure Laboratory  
Yale University, New Haven, CT 06511.

#### References

1. M. Gai, Z. Zhao, B.A. Brown, BAPS 32 (1987) 1579.
2. J.W. Olness, E.K. Warburton, D.E. Alburger, C.J. Lister and D.J. Millener, Nucl. Phys. A373 (1982) 13.
3. K. Neubeck, H. Schober, H. Waffler, Phys. Rev. C 10 (1974) 320.

Table I

$^{18}\text{N}$  beta decay branching ratios and logft

<u>Level</u>		<u>EXPT</u>		<u>MK<sup>a)</sup></u>		<u>MK1<sup>a)</sup></u>		<u>MWK<sup>b)</sup></u>	
<u>J</u>	<u>E<sup>x</sup></u>	<u>BR(%)</u>	<u>logft</u>	<u>BR</u>	<u>logft</u>	<u>BR</u>	<u>logft</u>	<u>BR</u>	<u>logft</u>
$1^-_3$	7.62	6.79(46)	5.21	3.1	5.77	1.0	6.30	1.0	6.03
$1^-_4$	8.04	1.82(19)	5.65	0.9	6.17	0.3	6.72	1.4	5.53

a) from reference 2.

b) B.A. Brown, private communication.



W.-T.Chou, R. Aryaeinejad, W.A. Olivier, and Wm.C. McHarris

The in-beam  $\gamma$ -ray spectra of odd-odd nuclei are less complex than anticipated. This comes about because heavy-ion reactions populate only a limited number of the available high spin states in the nuclei.<sup>1</sup> Once such "klokast" states are populated, the subsequent  $\gamma$  decay will preferentially feed into similar states, ultimately populating a select subset of the lower-lying states. During recent years, in the study of superdeformed bands it has been reported that these bands in odd-mass nuclei<sup>2</sup> receive greater population than those in even-even nuclei,<sup>3</sup> possibly because of a reduction in the pairing brought about by the odd nucleon. Thus superdeformed bands may receive even greater population in odd-odd nuclei.

We elected to study the odd-odd nucleus,  $^{176}\text{Re}_{101}$ , via in-beam  $\gamma$ -ray spectroscopy. We produced  $^{176}\text{Re}$  by the  $^{159}\text{Tb}(^{22}\text{Ne}, 5n\gamma)$  reaction in order to emphasize high-spin states, using a 108-MeV  $^{22}\text{Ne}$  beam from the NSCL K500 cyclotron. In Fig. 1 we show a partial  $^{176}\text{Re}$  level scheme constructed from our work; it includes the two most intensely populated rotational bands. Our  $\gamma$ - $\gamma$ -t coincidence spectra show these two rotational bands feeding into a state having a half-life of  $55 \pm 5$  ns, with this state deexciting by a 121.20-108.27-keV  $\gamma$ - $\gamma$  cascade. Unfortunately, the transitions feeding into the metastable state are not clear at present.

The rotational band shown on the right side of the level scheme is the  $1/2^-$ - $1/2^-$  doubly-decoupled band reported by Davidson et al.<sup>4</sup> in  $^{176,178}\text{Re}$ . It can be interpreted as the negative-signature splitting of a band formed by coupling the  $\pi(h_{9/2})1/2^- [541^+]$  and  $\nu(p_{3/2})1/2^- [521^+]$  states. The band-head is believed to be  $3^+$  although the  $5^+ \rightarrow 3^+$  transition was observed neither by Davidson et al. nor by us.

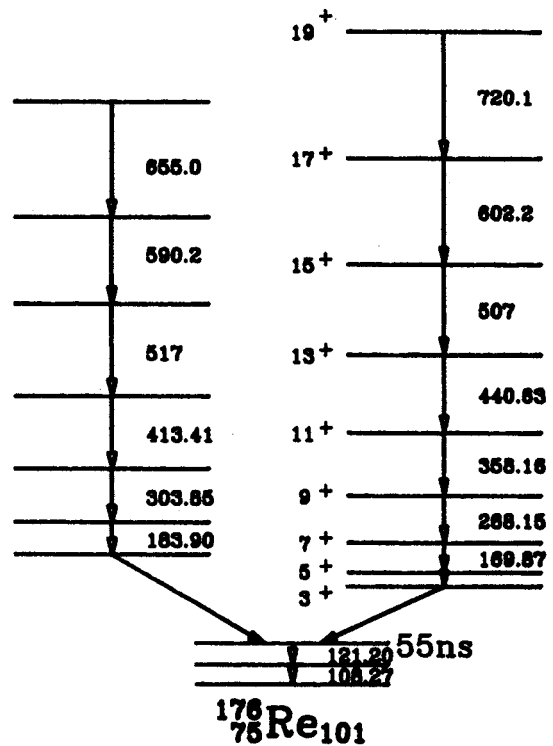


Fig. 1. Partial level scheme of  $^{176}\text{Re}$ .

The spacings in the other band, placed on the left side of the level scheme, indicate that it is a  $\Delta I=2$  band. However, since this band has almost the same energy as a  $1/2^-$  decoupled band in  $^{177}\text{Re}$ , we must demonstrate that it belongs in  $^{176}\text{Re}$ . In addition to excitation-function considerations, we present the following arguments: In our  $\gamma$ - $\gamma$ -t coincidence spectra, gating on transitions in either of the doubly-decoupled bands vs the 108.27-121.20-keV cascade produces the 55-ns half-life curve; gating on transitions in a decoupled band vs other transitions or transitions in the other decoupled band produces only a prompt peak, eliminating the possibility of background-subtraction artifacts. Also, preliminary results from experiments producing  $^{174}\text{Re}$ <sup>5</sup> show two similar doubly-decoupled bands having very similar energies; these cannot easily be

confused with  $^{177}\text{Re}$ . The very phenomenon of decoupled, rotationally-aligned bands means that the bands exhibit the rotational spectra of the core<sup>6</sup>; since  $^{176}\text{Re}$  and  $^{177}\text{Re}$  have the same core, similar spacings should be expected.

We also analyzed the continuum  $\gamma$ -ray spectrum for evidences of large deformation. In Fig. 2 we show three cuts perpendicular to the diagonal in the symmetrized  $E_{\gamma 1} - E_{\gamma 2}$  matrix. These cuts correspond to the energies 400, 904, and 1120 keV. The matrix was unfolded and uncorrelated  $\gamma$  rays were subtracted by the method of Andersson et al.<sup>7</sup> The dynamic moment of inertia<sup>2</sup>, was deduced from the width of the valley [width =  $8M^2 / \langle \omega^2 \rangle$ ], yielding values of 36, 53, and  $67 \text{ MeV}^{-1}$ , respectively, for the 400-, 904-, and 1120-keV regions. Calculating deformations from moments of inertia is somewhat uncertain, since this requires a detailed knowledge of the flow pattern within the nucleus. However, these moments of inertia correspond roughly to  $\beta$  values of 0.30, 0.35, and 0.40 in the three energy regions. Both the moment of inertia and the rough  $\beta$  value for the 1200-keV region can be construed as indicating "superdeformation," not so strong as in the  $^{152}\text{Dy}$  region, but comparable to that of the odd-mass Nd isotopes.<sup>2</sup> Note also the very pronounced ridges in the higher-energy cuts. These are consistent with specific groups of high- $j$  (decoupled, highly-aligned) states carrying much of the intensity.

The analysis of this experiment is still in progress. Angular-distribution measurements will be important in determining the multipolarity of the transitions.

#### References

1. M.F. Slaughter, R.A. Warner, T.L. Khoo, W. H. Kelly, and Wm. C. McHarris, Phys. Rev. C 29, 114 (1984).

2. E.M. Beck, F.S. Stephens, J.C. Bacelar, M.A. Deleplanque, R.M. Diamond, J.E. Draper, C. Duyar, and R.J. McDonald, Phys. Rev. Lett. 58, 2182 (1987).
3. P.J. Twin, B.M. Nyako, A.H. Nelson, J. Simpson, M.A. Bentley, H.W. Cranmer-Gordon, P.D. Forsyth, D. Howe, A.R. Mokhtar, J.K. Morrison, J.F. Sharpey-Schafer, and G. Slettin, Phys. Rev. Lett. 57, 811 (1986).
4. J. Davidson, M. Davidson, M. Debray, G. Falcone, D. Hojman, A.J. Kreiner, I. Mayans, C. Pomar, and D. Santos, Z. Phys. A 324, 363 (1986).
5. W.A. Olivier, R. Aryaeinejad, W.-T. Chou, and Wm. C. McHarris, MSU Cyclotron Laboratory Annual Report for 1987, pg. 106.
6. F.S. Stephens, Rev. Mod. Phys. 47, 43 (1975).
7. O. Andersen, J.D. Garrett, G.B. Hagemann, B. Herskind, D.L. Hillis, and L.L. Riedinger, Phys. Rev. Lett. 43, 687 (1979).

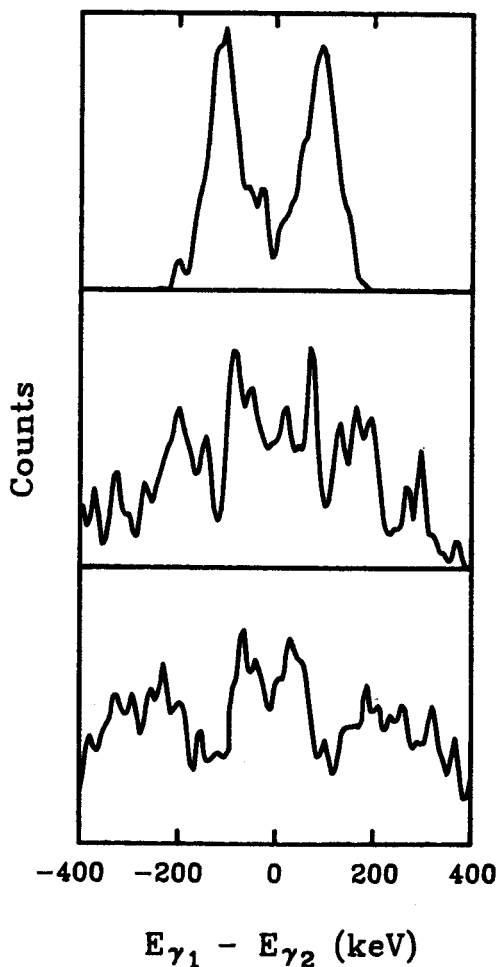


Fig. 2. Cuts perpendicular to the diagonal in the symmetrized  $E_{\gamma 1} - E_{\gamma 2}$  matrix at 4 keV/channel. Top: 400-keV region. Middle: 904-keV region. Bottom: 1120-keV region.

W.A. Olivier, W.-T. Chou, R. Aryaeinejad, and Wm.C. McHarris

MSU-88-063

The study of odd-odd neutron deficient Re nuclei has continued at NSCL with an investigation of the structure of rotational bands in  $^{174}\text{Re}$ .<sup>1</sup> Interest in odd-odd nuclei in this region has increased in the last few years. This can be attributed to several factors.

First, it was noted that heavy-ion reactions, while bringing large amounts of angular momentum into the system, tend to populate only a small fraction of the levels available.<sup>2</sup> The excited nuclei tend to "lock in" to specific rotational bands to de-excite. This simplifies the  $\gamma$ -ray spectrum to the point where analysis is tractable. It was also noted that these "klokast" bands tend to be built on particle couplings that demonstrate highly-aligned character.<sup>3</sup>

Second, the observation of "doubly-decoupled" bands in this region by Kreiner et al.<sup>4</sup> has prompted interest in a study of the residual interaction between the proton and neutron in medium-mass systems. These nuclei are excellent candidates for such a study because of this doubly-decoupled character. The structure of the system is represented schematically Fig. 1. One can imagine the odd proton and the odd neutron coupled to a prolate core. The odd particles orbiting the core both occupy  $\Omega=1/2$  orbitals; in other words, they are highly-aligned in the rotational system. It has been demonstrated in some systems these odd nucleons are essentially independent of the core structure and motion. This means the proton-neutron residual interaction can be studied apart from the coupling of the individual nucleons to the core.

Third, there is the possible existence of superdeformation in this region. Our analysis of data for  $^{176}\text{Re}$  shows evidence for this phenomenon.<sup>5,6</sup> The odd-odd nuclei have an

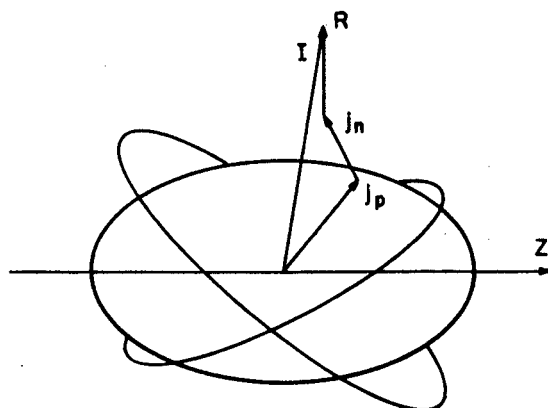


Fig. 1: A pictorial illustration of the coupling of the odd particles to a prolate core.  $Z'$  denotes the symmetry axis;  $R$ , the rotational angular momentum;  $j_{p,n}$  and  $I$ , the particle and total angular momenta, respectively.

excellent opportunity to display this type of behavior since the odd particles can block the pairing of both the neutrons and the protons in these nuclei.

The investigation of band structure in  $^{174}\text{Re}$  was done in-beam with standard  $\gamma$ - $\gamma$ -t coincidence parameters. The reaction to form the  $^{174}\text{Re}$  was  $^{159}\text{Tb}(^{20}\text{Ne}, 5n\gamma)^{174}\text{Re}$  at 114 MeV total beam energy. The target was a self-supporting foil rolled to a thickness of  $\approx 1.0$  mg/cm<sup>2</sup>. Two 15%-efficient intrinsic Ge detectors were positioned at  $\pm 90^\circ$  to the beam. One detector was operated in a compton-suppressed mode with an 8" NaI(Tl) annulus and located  $\approx 25$  cm from the target. The other Ge detector was bare and located  $\approx 12$  cm from the target. Seven 3x3" NaI(Tl) detectors were also clustered about the target at various angles and distances and used as a multiplicity filter.

Examples of typical spectra are shown in Fig. 2. The compton-shielded detector was used to determine the energies of the transitions, while the bare detector was generally used for gates.

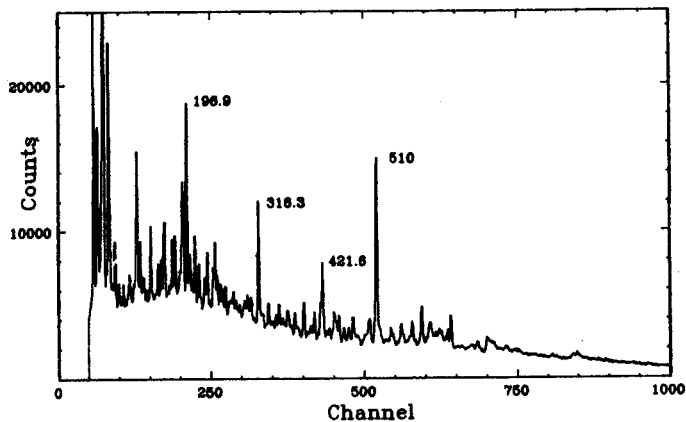


Fig. 2a: Ungated coincidence spectrum of the Compton-suppressed detector for  $^{174}\text{Re}$ .

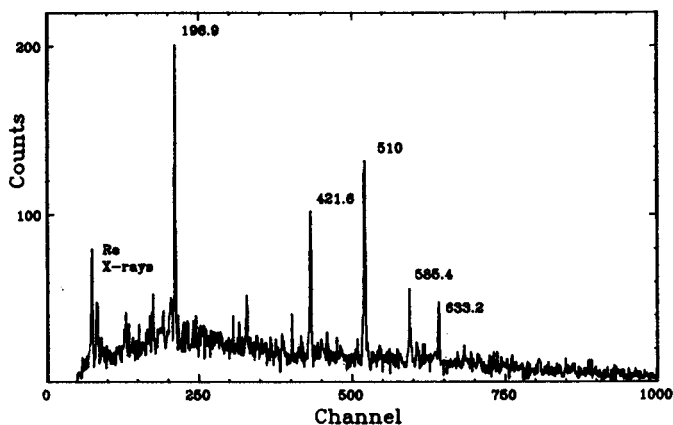


Fig. 2b. Coincidence spectrum gated on the 316.3 keV transition in  $^{174}\text{Re}$ .

Prior to this investigation, no levels had been characterized in  $^{174}\text{Re}$ . To this point in the analysis, five rotational bands consisting of more than thirty levels have been identified. A tentative level scheme is shown in Fig. 3.

The ground state of  $^{174}\text{Re}$  appears to be a  $4^-$  level formed by the coupling of the  $\pi(h_{9/2})1/2^- [541]$  and  $\nu(i_{13/2})7/2^+ [633]$  states. All of the observed bands in the level scheme appear to feed this band through the 23-ns metastable state at 343.6 keV. The second band from the right is built on a coupling of the  $\pi(d_{5/2})5/2^+ [402]$  and  $\nu(i_{13/2})7/2^+ [633]$  states. It is a well-behaved  $\Delta I=1$  rotational band with spins extending to  $13M$ . The third rotational band that has been characterized to date is the doubly-decoupled band. It is built on a coupling of the  $\pi(h_{9/2})1/2^- [541]$  and  $\nu(p_{3/2})1/2^- [521]$  states. This is the same coupling that is observed in the heavier Re isotopes and leads one to believe that it should continue to much more neutron-deficient systems.

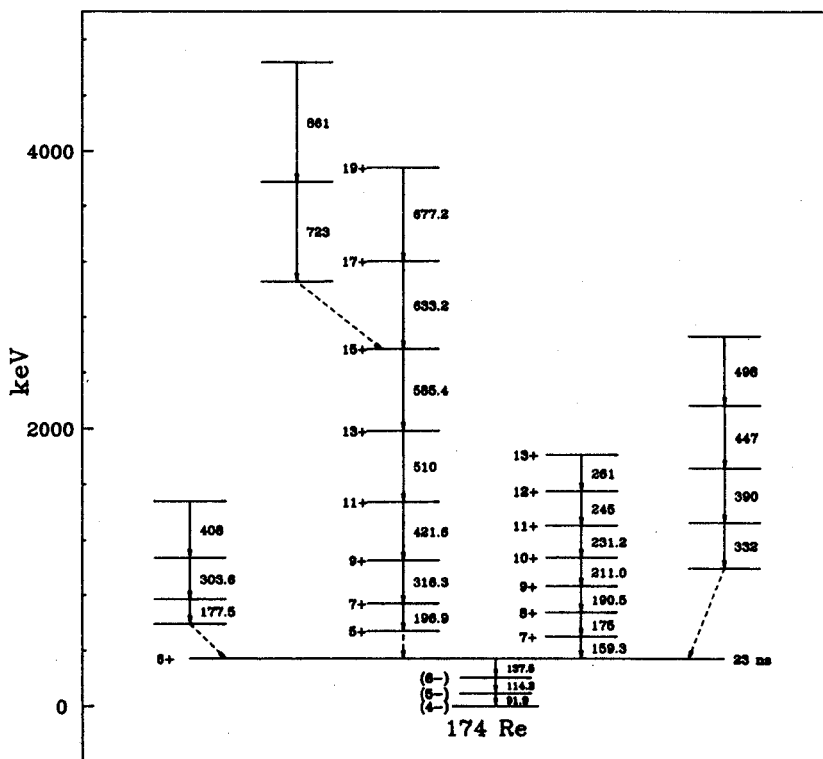


Fig. 3. A partial level scheme of  $^{174}\text{Re}$ .

## References

1. W.A. Olivier, W.-T. Chou, R. Aryaeinejad, and Wm.C. McHarris, Cyclotron Laboratory Annual Report 1986, NSCL, Michigan State University, p.87 (1987).
2. M.F. Slaughter, R.A. Warner, T.L. Khoo, W.H. Kelly, and Wm.C. McHarris, Phys. Rev. C29, 114 (1984).
3. Wm. C. McHarris, W.-T. Chou, J. Kupstas-Guido, and W.A. Olivier, in Nuclei Off the Line of Stability, ed. by R.A. Meyer and D.S. Brenner, American Chemical Society Symposium Series #324 (1986), p. 329.
4. A.J. Kreiner, D.E. Digregorio, A.J. Fendrik, J. Davidson, and M. Davidson, Nucl. Phys. A432, 451 (1985).
5. R. Aryaeinejad, W.-T. Chou, W.A. Olivier, and Wm.C. McHarris, NSCL report MSUCL-617, submitted to Phys. Lett. (1988).
6. W.-T. Chou, R. Aryaeinejad, W.A. Olivier, and Wm.C. McHarris, Cyclotron Laboratory Annual Report for 1987, pg. 104.

I. Ahmad<sup>a</sup>, Z.M. Koenig<sup>b</sup>, and Wm.C. McHarris

The odd-odd actinide nucleus  $^{250}\text{Bk}$  is unique in that its states can be probed in a number of complementary ways. It is the daughter of 276-d  $^{254}\text{Es}^g$ , a  $J^\pi = 7^+$  nuclide whose  $\alpha$  decay populates a number of high-spin rotational bands in it. The low-spin ( $2^+$ ) isomer  $^{254}\text{Es}^m$  decays primarily by  $\beta^-$  emission, but it has a 0.33%  $\alpha$  branch that populates low-spin bands in  $^{250}\text{Bk}$ . In addition, the recent availability of  $^{249}\text{Bk}$  in large enough quantities for useful targets has made transfer reactions, such as  $^{249}\text{Bk}(d,p)^{250}\text{Bk}$ , and neutron-capture  $\gamma$ -ray studies feasible; these populate more or less independent sets of states in  $^{250}\text{Bk}$ . Thus, for this particular heavy odd-odd nuclide, we have more and more varied information than is available for most lighter odd-odd systems. In our present investigation we have studied  $^{254}\text{Es}^g$  decay by  $\alpha$ ,  $\gamma$ -ray, and conversion- $e^-$  spectroscopy, complemented by the (d,p) reaction. Our results, together with existing data from the decay<sup>1</sup> of  $^{254}\text{Es}^m$  and neutron-capture  $\gamma$ -ray studies,<sup>2</sup> have enabled us to identify and analyze many states and bands in  $^{250}\text{Bk}$ , including experimental triplet-singlet coupling separations for four distinct band pairs.

The  $^{254}\text{Es}^g$  sample, prepared in the ORNL High-Flux Isotope Reactor by successive neutron capture on  $^{239}\text{Pu}$ , was purified by standard chemical procedures, then further purified in the ANL double electromagnetic isotope separator by depositing it as 200-eV ions onto a 200- $\mu\text{g}/\text{cm}^2$  Al foil. This "massless" source contained  $6.5 \times 10^6$  dpm, three orders of magnitude more intense than the source used for the original  $^{254}\text{Es}^g$  studies.<sup>3</sup>

Details of our spectroscopic studies are given elsewhere,<sup>4</sup> but we include here two

examples of spectra. Fig. 1 shows the high-energy portion (populating low-lying states in  $^{250}\text{Bk}$ ) of the  $\alpha$  spectrum taken with the ANL double-focusing magnetic spectrometer. Fig. 2 shows a "wide-range"  $\gamma$ -ray spectrum:  $\gamma$ -rays (planar Ge detector) in coincidence with all  $\alpha$  particles (Si  $\alpha$  detector).

Our resulting decay scheme is shown in Fig. 3. We have characterized 22 states in seven rotational bands populated by high-spin  $^{254}\text{Es}^g$ ; an additional 17 states are shown at the left of Fig. 3. Twelve mostly different lower-spin states are populated by the  $\alpha$  decay of  $^{254}\text{Es}^m$ ; these are shown in Fig. 4 for comparison.

The band properties are summarized in Table I, where they are compared with calculated properties for bands expected in  $^{250}\text{Bk}$ . Energies of states in these bands are characterized by a slightly extended rotational equation,

$$E_J = E_0 + \left(\frac{M}{2}\right)J(J+1) + BJ^2(J+1)^2$$

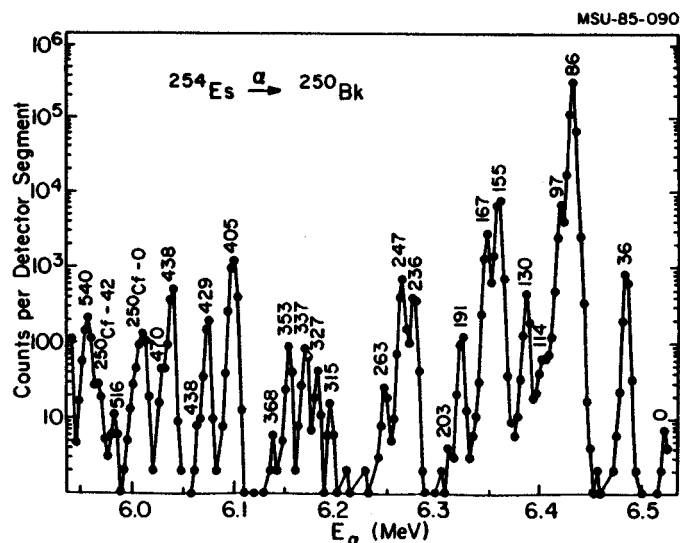


Fig. 1:  $\alpha$ -particle spectrum from the decay of  $^{254}\text{Es}^g$  taken in the ANL magnetic spectrometer. (High-energy portion.)

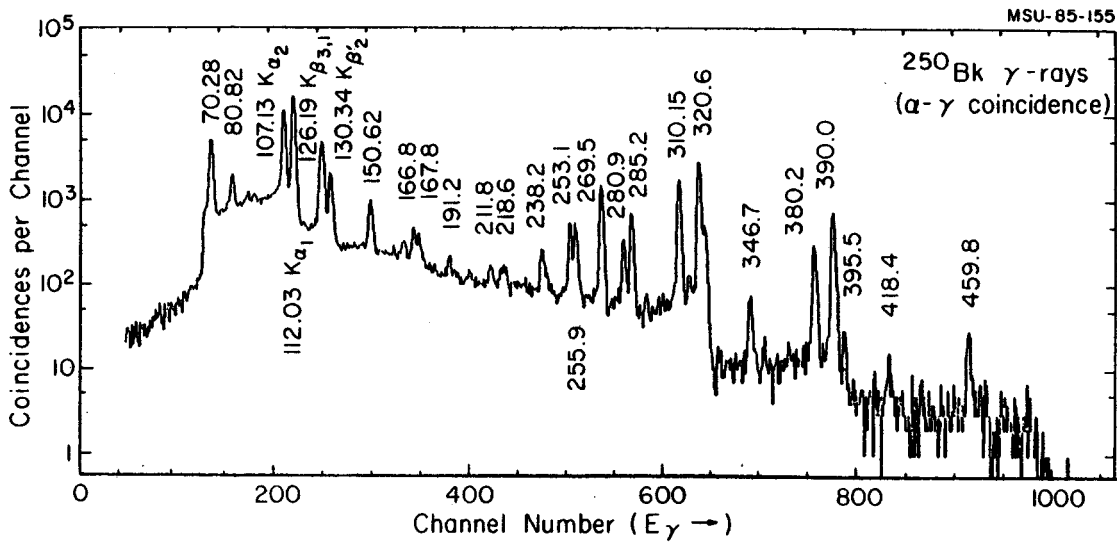


Fig. 2:  $^{250}\text{Bk}$   $\gamma$ -rays in coincidence with  $\alpha$ -particles from  $^{254}\text{Es}^g$  decay.

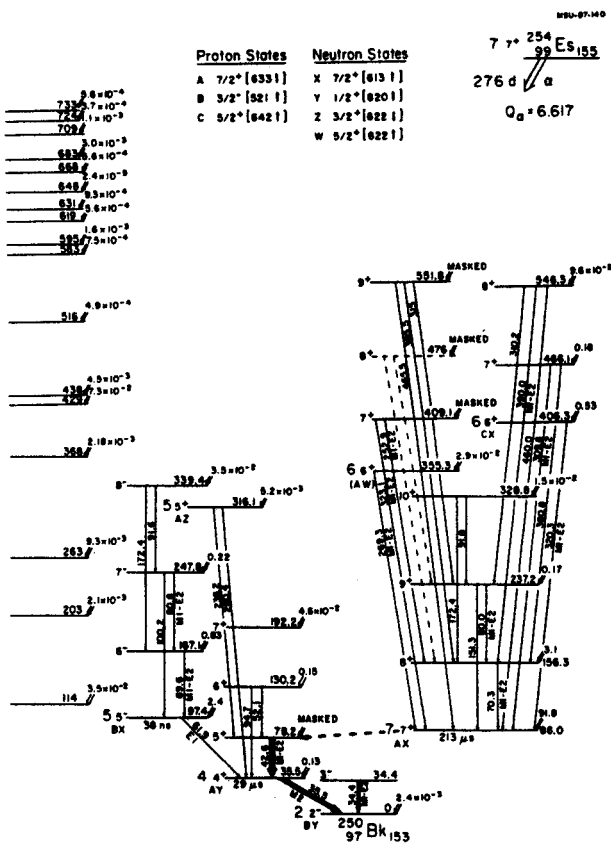


Fig. 3. Decay scheme of  $^{254}\text{Es}^g$ .

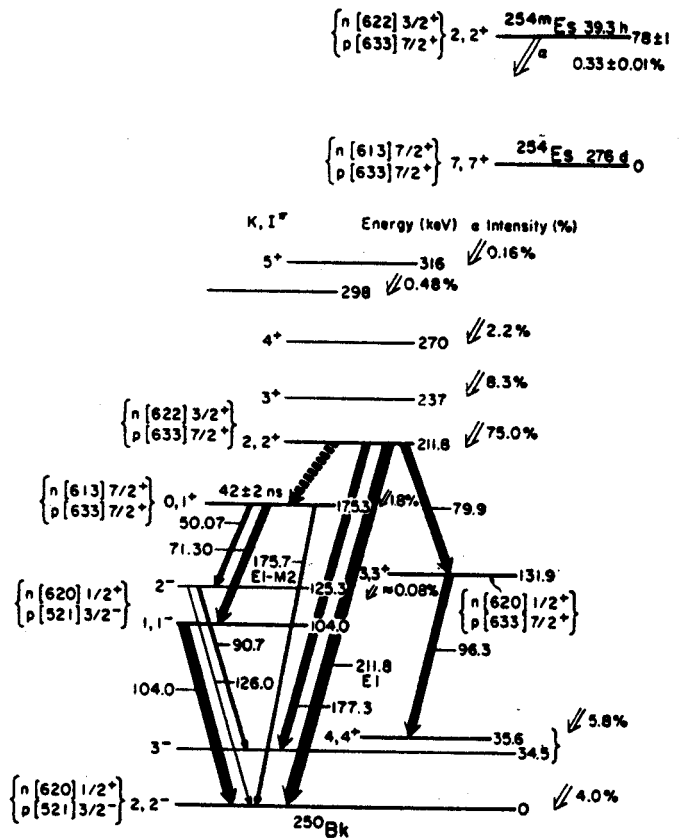


Fig. 4. Decay scheme of  $^{254}\text{Es}^m$  (from Ref. 1).

Table I. Properties of Rotational Bands in  $^{250}\text{Bk}$

Proton States				
Neutron States	$7/2^+[633+]$	$3/2^-[521+]$	$5/2^+[642+]$	$1/2^+[400+]$
	<u>Predicted Properties</u>			
$1/2^+[620+]$	$K^\pi = 4^+(3^+)$ $E_x = 0 \text{ keV}$ $\hbar^2/2 = 4.25 \text{ keV}$ B = +	$2^-(1^-)$ 22	$3^-(2^+)$ 329	$1^+(0^+)$ 345
$7/2^+[613+]$	$7^+(0^+)$ 79 4.29 +	$5^-(2^-)$ 101 5.80 -	$6^+(1^+)$ 408 5.24 +	$4^+(3^+)$ 424 6.00 -
$3/2^+[622+]$	$2^+(5^+)$ 193 4.40 +	$0^-(3^-)$ 215 6.00 -	$1^+(4^+)$ 522 5.50 +	$1^+(2^+)$ 538 6.20 -
$11/2^-[725+]$	$9^-(2^-)$ 370 3.82 +	$7^+(4^+)$ 392 4.98 +	$8^-(3^-)$ 699 4.56 +	$6^-(5^-)$ 715 5.12 +
$5/2^+[622+]$	$6^+(1^+)$ 537 4.32 +	$4^-(1^-)$ 559 5.84 -	$5^+(0^+)$ 866 5.27 +	$3^+(2^+)$ 882 6.04 -
	<u>Experimental Properties</u>			
$1/2^+[620+]$	$4^+(3^+)$ 35.5(131.9) 4.26 +	$2^-(1^-)$ 5.73 -		
$7/2^+[613+]$	$7^+(0^+)$ 86.0(175.3) 4.40 +	$5^-$ 97.4 5.75 -	$6^+$ 406.3 4.27 +	
$3/2^+[622+]$	$2^+(5^+)$ 211.8(316.1) 4.20 +			
$11/2^-[725+]$				
$5/2^+[622+]$	$6^+$ 355.3 3.84 +?			

because of the severe coriolis coupling in many of the bands. Expansion of the coriolis terms in a simple perturbation series yields a negative term in  $J(J+1)$  and a positive term in  $J^2(J+1)^2$ . Thus, states having large coriolis matrix elements (states originating from large-j spherical orbitals) show large effective moments of inertia (smaller than usual values of  $\hbar^2/2$ ) and positive, relatively large B terms (as opposed to centrifugal stretching, which produces a small, negative B term). The agreements are remarkable, considering the complexity of the situation, demonstrating that these odd-mass properties carry over very well into the odd-odd states.

The combined data also allow experimental determination of the triplet-singlet separation for four distinct band pairs, the most known in a single odd-odd nucleus. These are listed in Table II both as raw band-head separations and as splittings after the K dependence has been removed.<sup>5</sup> These should provide new impetus to calculating these splittings, which thus far have been only semi-successful.<sup>6-8</sup>

Our analyses of results from the  $^{249}\text{Bk}(d,p)^{250}\text{Bk}$  reaction are not so complete, but they complement the  $\alpha$ -decay studies. Spectra were taken at  $90^\circ$  and  $125^\circ$  in the ANL magnetic spectrometer, using a 15-MeV d beam from the Tandem Van de Graaff. We show the  $125^\circ$  spectrum in Fig. 5. In addition, Hoff et al.<sup>2</sup> have identified nine bands in  $^{250}\text{Bk}$  from  $^{249}\text{Bk}(n,\gamma)$  studies. The total wealth of information should allow us to perform detailed calculations in the near future. We have already performed extensive interacting boson-fermion-fermion calculations for odd-odd Re nuclei,<sup>9</sup> and these reproduce the coriolis distortions there very well. Thus, although a larger basis set will require messier calculations for the Bk region, we expect similar agreement. The triplet-singlet splitting are not so straightforward, but a combination of our methods with those developed by Hoff et al., show provide a good point of departure.

Table II. Triplet-Singlet Splittings in  $^{250}\text{Bk}$

Proton State	Neutron State	Band-head Separation	Triplet-Singlet Splitting
$3/2^-[521+]$	$1/2^+[620+]$	104.0 keV	109.7 keV
$7/2^+[633+]$	$1/2^+[620+]$	96.4	100.7
$7/2^+[633+]$	$7/2^+[613+]$	89.3 <sup>a</sup>	120.1 <sup>a</sup>
$7/2^+[633+]$	$3/2^+[622+]$	104.3	116.9

<sup>a</sup>The singlet coupling has  $K^\pi = 0^+$ , with a  $J = 1$  band-head; the splitting does not take into account the odd-even shifts in this band.



- a. Physics Division, Argonne National Laboratory, Argonne, Ill.
- b. KMS Fusion, Ann Arbor, Mich.

References

1. I. Ahmad, H. Diamond, J. Milsted, J. Lerner, and R.K. Sjoblom, Nucl. Phys. A208, 287 (1973).
2. R.W. Hoff, J. Kern, R. Piepenbring, and J.B. Boisson, Capture Gamma-Ray Spectroscopy and Related Topics -- 1984, ed. by S. Raman, AIP Conference Proceedings, No. 125, p. 274 (1985).
3. Wm.C. McHarris, F.S. Stephens, F. Asaro, and I. Perlman, Phys. Rev. 144, 1031 (1966).
4. I. Ahmad, Z.M. Koenig, and Wm.C. McHarris, MSUCL-612, submitted to Phys. Rev. C.
5. J.P. Davidson, Collective Models of the Nucleus, (Academic Press, New York, 1968), p. 86.
6. N.D. Newby, Phys. Rev. 125, 2063 (1962).
7. H.D. Jones, N. Onishi, T. Hess, and R.K. Sheline, Phys. Rev. C 3, 529 (1971).
8. P.C. Sood and R.N. Singh, Nucl. Phys. A419, 547 (1984).
9. W.-T. Chou, Wm. C. McHarris, and Olaf Scholten, MSCL-611, accepted for publ. in Phys. Rev. C; see also contribution on pg. 123 in this Annual Report.

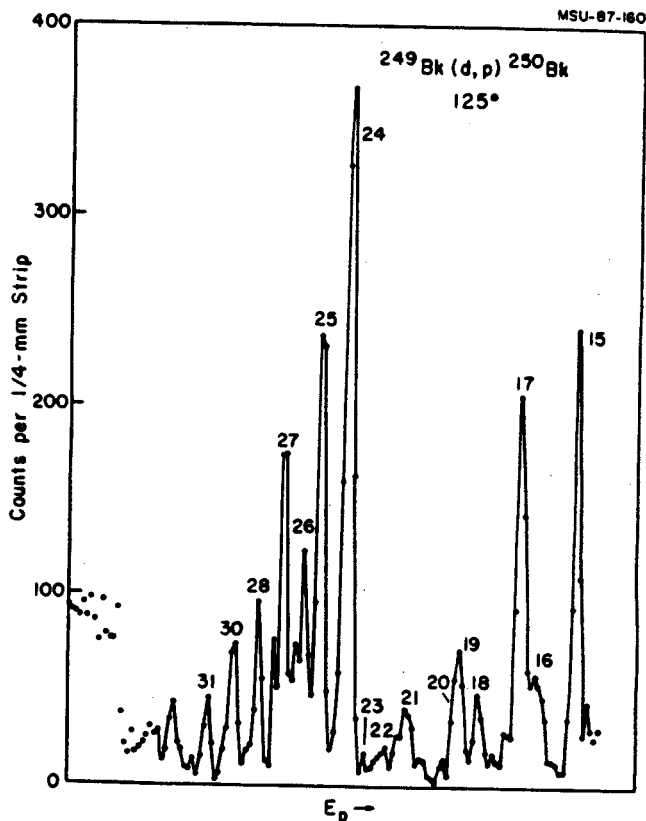
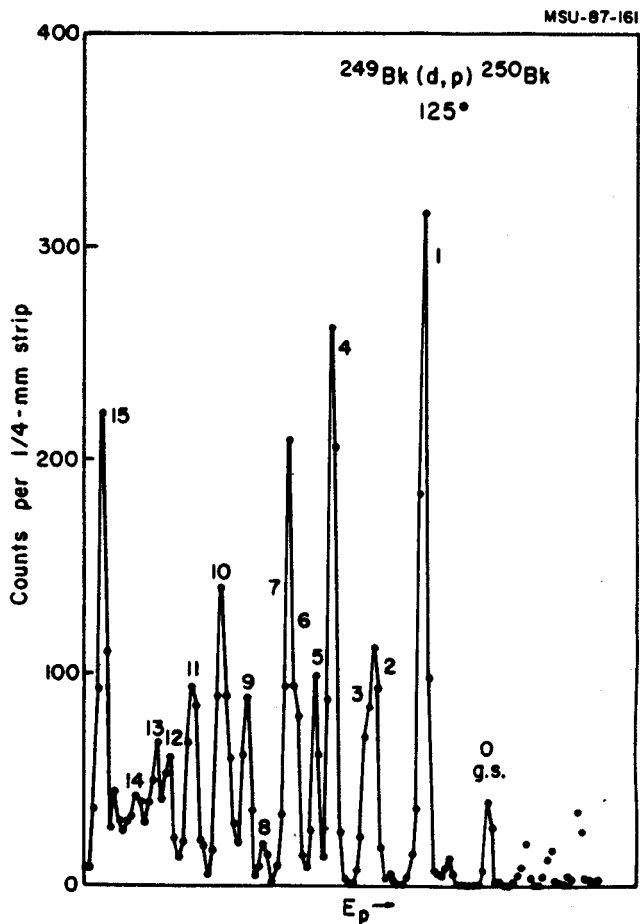


Fig. 5.  $^{249}\text{Bk}(d,p)^{250}\text{Bk}$  spectrum taken at 125°.

Table I. Properties of Rotational Bands in  $^{250}\text{Bk}$

Proton States				
Neutron States	$7/2^+[633+]$	$3/2^-[521+]$	$5/2^+[642+]$	$1/2^+[400+]$
	<u>Predicted Properties</u>			
$1/2^+[620+]$	$K^\pi = 4^+(3^+)$ $E_x = 0 \text{ keV}$ $\hbar^2/2 = 4.25 \text{ keV}$ $B = +$	$2^-(1^-)$ 22	$3^+(2^+)$ 329	$1^+(0^+)$ 345
		5.54	5.03	5.72
$7/2^+[613+]$	$7^+(0^+)$ 79 4.29 +	$5^-(2^-)$ 101 5.80 -	$6^+(1^+)$ 408 5.24 +	$4^+(3^+)$ 424 6.00 -
$3/2^+[622+]$	$2^+(5^+)$ 193 4.40 +	$0^-(3^-)$ 215 6.00 -	$1^+(4^+)$ 522 5.50 +	$1^+(2^+)$ 538 6.20 -
$11/2^-[725+]$	$9^-(2^-)$ 370 3.82 +	$7^+(4^+)$ 392 4.98 +	$8^-(3^-)$ 699 4.56 +	$6^-(5^-)$ 715 5.12 +
$5/2^+[622+]$	$6^+(1^+)$ 537 4.32	$4^-(1^-)$ 559 5.84	$5^+(0^+)$ 866 5.27	$3^+(2^+)$ 882 6.04
	<u>Experimental Properties</u>			
$1/2^+[620+]$	$4^+(3^+)$ 35.5(131.9) 4.26 +	$2^-(1^-)$ 0(104.0) 5.73 -		
$7/2^+[613+]$	$7^+(0^+)$ 86.0(175.3) 4.40 +	$5^-$ 97.4 5.75 -	$6^+$ 406.3 4.27 +	
$3/2^+[622+]$	$2^+(5^+)$ 211.8(316.1) 4.20 +			
$11/2^-[725+]$				
$5/2^+[622+]$	$6^+$ 355.3 3.84 +?			

because of the severe coriolis coupling in many of the bands. Expansion of the coriolis terms in a simple perturbation series yields a negative term in  $J(J+1)$  and a positive term in  $J^2(J+1)^2$ . Thus, states having large coriolis matrix elements (states originating from large-j spherical orbitals) show large effective moments of inertia (smaller than usual values of  $\hbar^2/2$ ) and positive, relatively large B terms (as opposed to centrifugal stretching, which produces a small, negative B term). The agreements are remarkable, considering the complexity of the situation, demonstrating that these odd-mass properties carry over very well into the odd-odd states.

The combined data also allow experimental determination of the triplet-singlet separation for four distinct band pairs, the most known in a single odd-odd nucleus. These are listed in Table II both as raw band-head separations and as splittings after the K dependence has been removed.<sup>5</sup> These should provide new impetus to calculating these splittings, which thus far have been only semi-successful.<sup>6-8</sup>

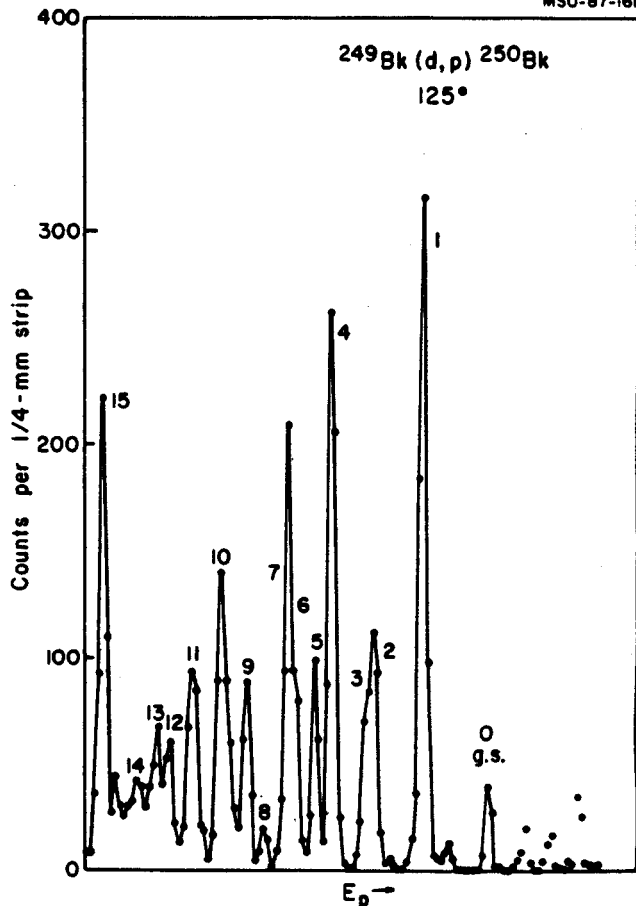
Our analyses of results from the  $^{249}\text{Bk}(d,p)^{250}\text{Bk}$  reaction are not so complete, but they complement the  $\alpha$ -decay studies. Spectra were taken at  $90^\circ$  and  $125^\circ$  in the ANL magnetic spectrometer, using a 15-MeV d beam from the Tandem Van de Graaff. We show the  $125^\circ$  spectrum in Fig. 5. In addition, Hoff et al.<sup>2</sup> have identified nine bands in  $^{250}\text{Bk}$  from  $^{249}\text{Bk}(n,\gamma)$  studies. The total wealth of information should allow us to perform detailed calculations in the near future. We have already performed extensive interacting boson-fermion-fermion calculations for odd-odd Re nuclei,<sup>9</sup> and these reproduce the coriolis distortions there very well. Thus, although a larger basis set will require messier calculations for the Bk region, we expect similar agreement. The triplet-singlet splitting are not so straightforward, but a combination of our methods with those developed by Hoff et al., show provide a good point of departure.

Table II. Triplet-Singlet Splittings in  $^{250}\text{Bk}$

Proton State	Neutron State	Band-head Separation	Triplet-Singlet Splitting
$3/2^-[521+]$	$1/2^+[620+]$	104.0 keV	109.7 keV
$7/2^+[633+]$	$1/2^+[620+]$	96.4	100.7
$7/2^+[633+]$	$7/2^+[613+]$	89.3 <sup>a</sup>	120.1 <sup>a</sup>
$7/2^+[633+]$	$3/2^+[622+]$	104.3	116.9

<sup>a</sup>The singlet coupling has  $K^\pi = 0^+$ , with a J = 1 band-head; the splitting does not take into account the odd-even shifts in this band.

MSU-87-161



- a. Physics Division, Argonne National Laboratory, Argonne, Ill.
- b. KMS Fusion, Ann Arbor, Mich.

## References

1. I. Ahmad, H. Diamond, J. Milsted, J. Lerner, and R.K. Sjoblom, Nucl. Phys. A208, 287 (1973).
2. R.W. Hoff, J. Kern, R. Piepenbring, and J.B. Boisson, Capture Gamma-Ray Spectroscopy and Related Topics -- 1984, ed. by S. Raman, AIP Conference Proceedings, No. 125, p. 274 (1985).
3. Wm.C. McHarris, F.S. Stephens, F. Asaro, and I. Perlman, Phys. Rev. 144, 1031 (1966).
4. I. Ahmad, Z.M. Koenig, and Wm.C. McHarris, MSUCL-612, submitted to Phys. Rev. C.
5. J.P. Davidson, Collective Models of the Nucleus, (Academic Press, New York, 1968), p. 86.
6. N.D. Newby, Phys. Rev. 125, 2063 (1962).
7. H.D. Jones, N. Onishi, T. Hess, and R.K. Sheline, Phys. Rev. C 3, 529 (1971).
8. P.C. Sood and R.N. Singh, Nucl. Phys. A419, 547 (1984).
9. W.-T. Chou, Wm. C. McHarris, and Olaf Scholten, MSCL-611, accepted for publ. in Phys. Rev. C; see also contribution on pg. 123 in this Annual Report.

MSU-87-160

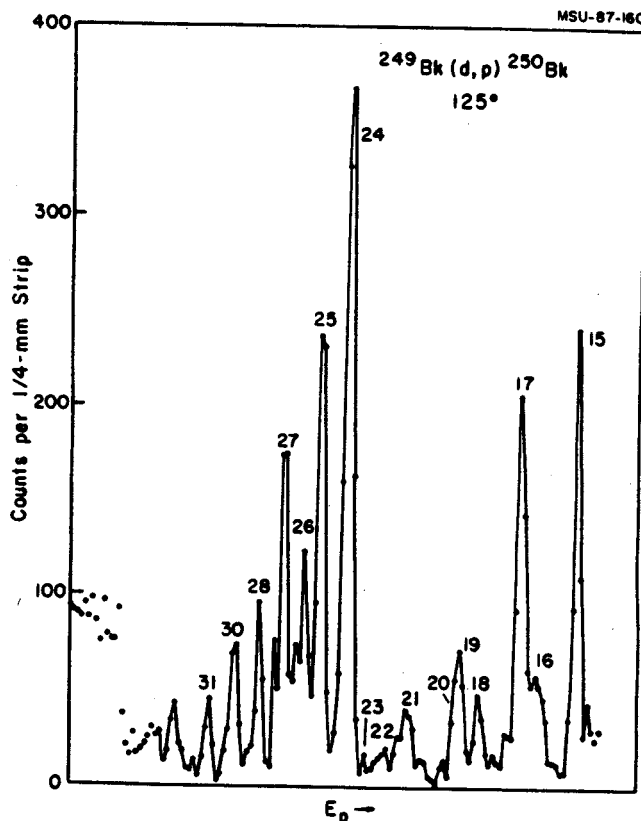


Fig. 5.  $^{249}\text{Bk}(d,p)^{250}\text{Bk}$  spectrum taken at  $125^\circ$ .

R. Aryaeinejad and Wm.C. McHarris

In-beam  $\gamma$ -ray spectroscopy was used to study states in the  $N = 80$  nucleus,  $^{139}\text{Pr}$ , via the  $^{140}\text{Ce}(p,2n\gamma)$  and  $^{139}\text{La}(\alpha,4n\gamma)$  reactions. This completes studies on the series of isotones,  $^{143}\text{Eu}_{80}$ ,  $^{141}\text{Pm}_{80}$ , and  $^{139}\text{Pr}_{80}$ , enabling us to investigate systematics of this region close to the  $N = 82$  closed shell. We have just completed calculations for states in these nuclei using the triaxial model,<sup>1</sup> which we discuss here. In addition, we are currently performing IBFA calculations,<sup>2,3</sup> which should be the basis for a forthcoming paper.

The experimental results for states in  $^{139}\text{Pr}$  are shown in Fig. 1 for the p-induced reaction and in Fig. 2 for the  $\alpha$ -induced reaction. A summary of the known states in the  $N = 80$  isotones is given in Fig. 3. For convenience of discussion, we discuss the states in three groups: 1) single-quasiparticle states, 2) negative-parity collective states, and 3) positive-parity collective states.

Single-Quasiparticle States  
In  $^{139}\text{Pr}$  one can expect to see evidence of

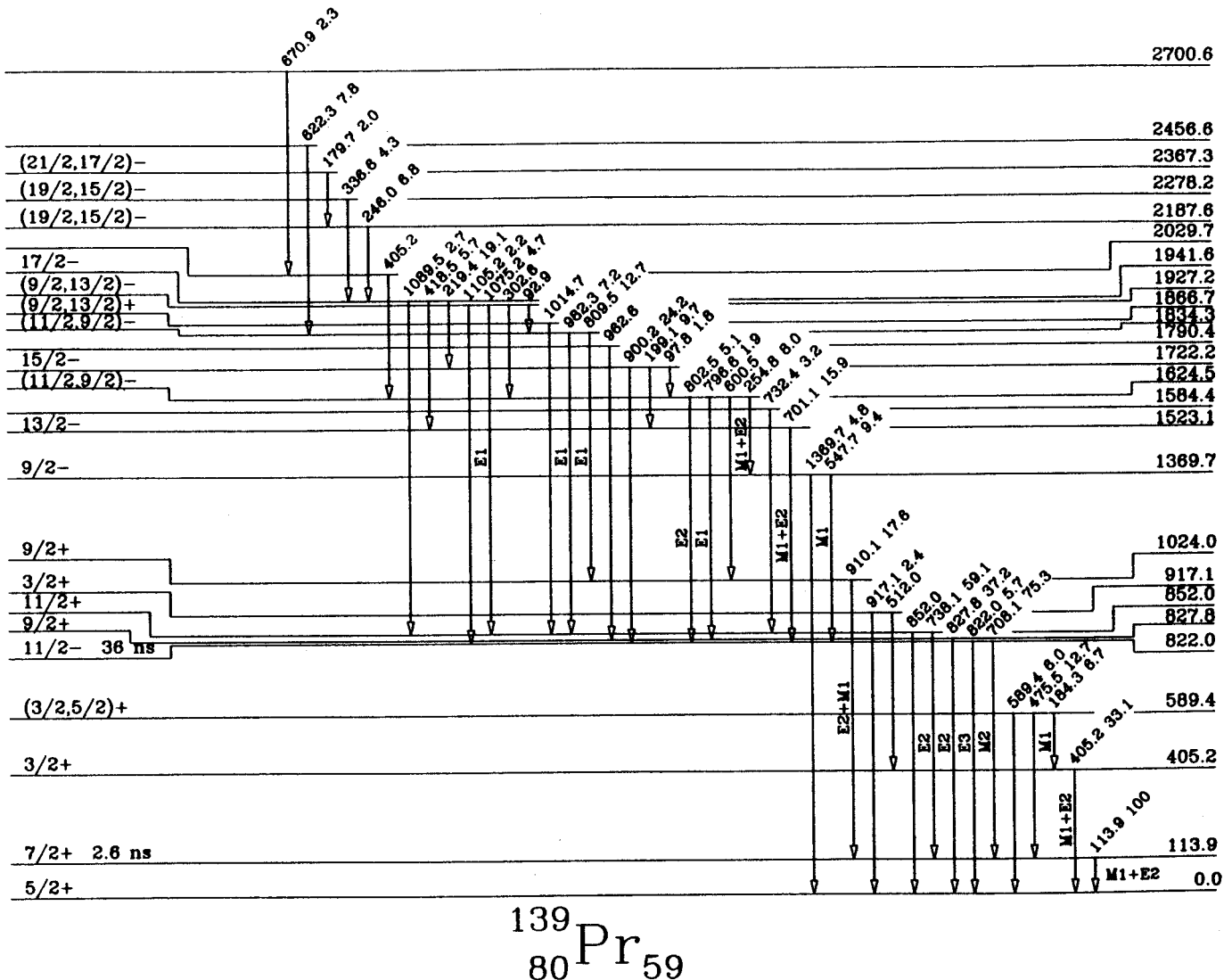


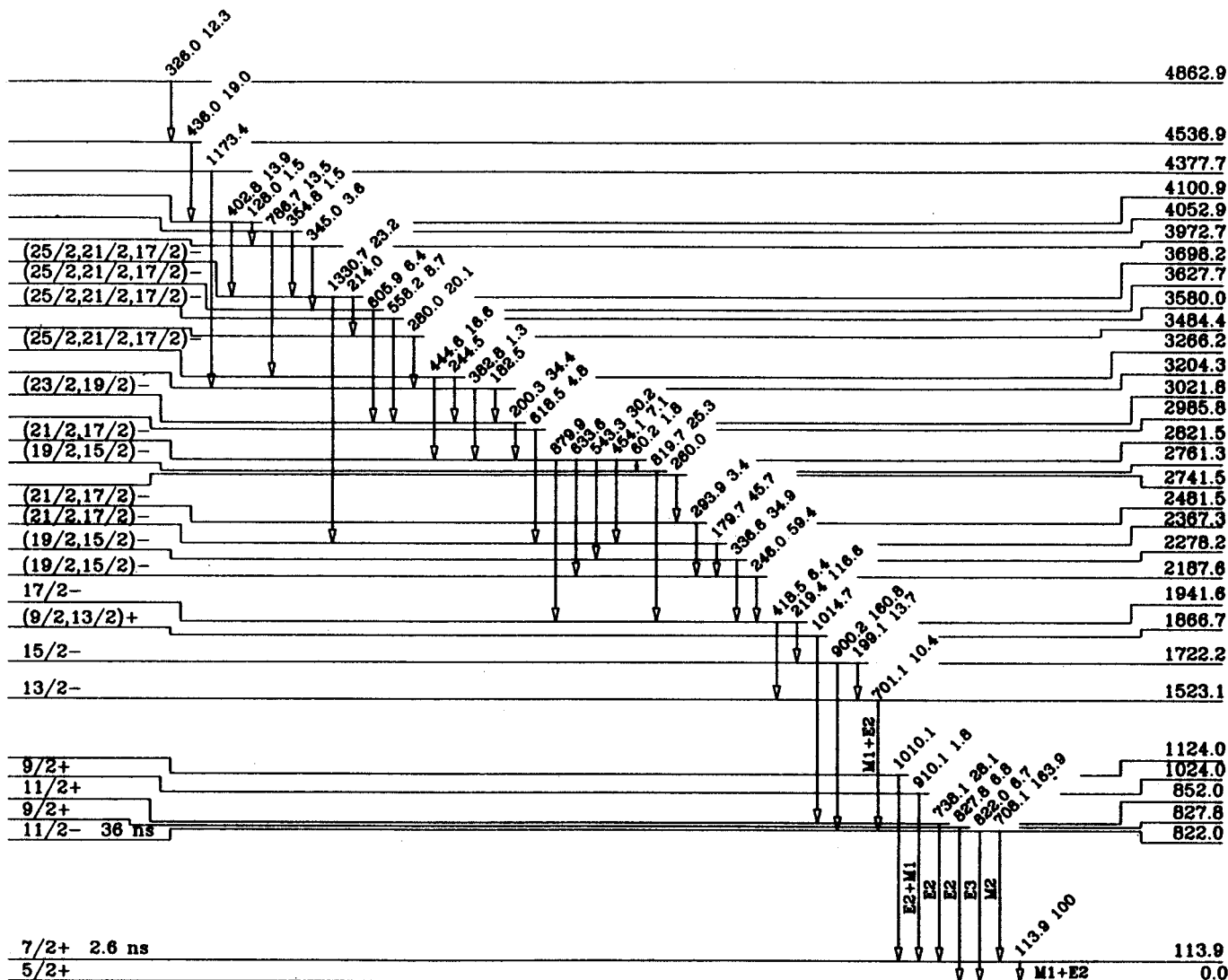
Fig. 1:  $^{139}\text{Pr}$  level scheme from the  $(p,2n\gamma)$  reaction.

all the available single-proton states between  $Z = 50$  and  $Z = 82$ . The most clearcut single-quasiparticle states are those at 0, 113.9, 405.2, and 822.0 keV. The ground state undoubtedly consists primarily of a single  $\pi d_{5/2}$  state outside the closed  $\pi g_{7/2}$  subshell, and the 113.9-keV state simply promotes a  $g_{7/2}$  proton into a  $d_{5/2}$  orbital, resulting in  $\pi g_{7/2} \pi d_{5/2}^2$ . The (p,t) reaction lends credence to such assignments, and the retarded M1 transition between the two states is characteristic of 1-

forbidden M1's between  $g_{7/2}$  and  $d_{5/2}$  states in a wide range of nuclei.

The state at 405.2 keV appears to contain much of the  $\pi d_{3/2}$  strength. The  $\pi d_{3/2}$  state has been observed at 403.8 keV in  $^{141}\text{Pm}$  but appears to be fragmented in  $^{143}\text{Eu}$ . On the other hand, our triaxial calculations predict a  $3/2^+$  state to lie at 280 keV as a  $\pi d_{3/2}$  core-coupled state.

The 822.0-keV state shows evidence of being the  $\pi h_{11/2}$  state. The M2 transition from this state to the 113.9-keV state is retarded



### $^{139}\text{Pr}_{59}$

Fig. 2:  $^{139}\text{Pr}$  level scheme from the  $(\alpha, 4n\gamma)$  reaction.

comparable to similar M2's in this region, and the E3 is slightly enhanced, consistent with E3's in this region (implying some octupole deformation or triaxiality).

The position of the  $\pi s_{1/2}$  state is not so clear, but it is probably fragmented and contributes to several states near 1 MeV.

### Negative-Parity Collective States

Within the framework of the triaxial model, the negative-parity states are expected to consist primarily of the  $\pi h_{11/2}$  state coupled to

a  $^{138}\text{Ce}$  triaxial core. The most likely core state, the first  $2^+$  excited state, lies at  $\approx 790$  keV. The low-lying ( $\pi h_{11/2} \times 2_1^+$ ) states should be rather pure configurations, and their center of gravity should lie near 1612 keV. The 1369.7-, 1523.1-, and 1722.2-keV states, all of which deexcite through the 822.0-keV state, very likely are three such states. They exhaust the primary strength of the  $9/2^-$ ,  $13/2^-$ , and  $15/2^-$  components of the configuration. And the 1624.5-keV state is a candidate for the  $11/2^-$  component.

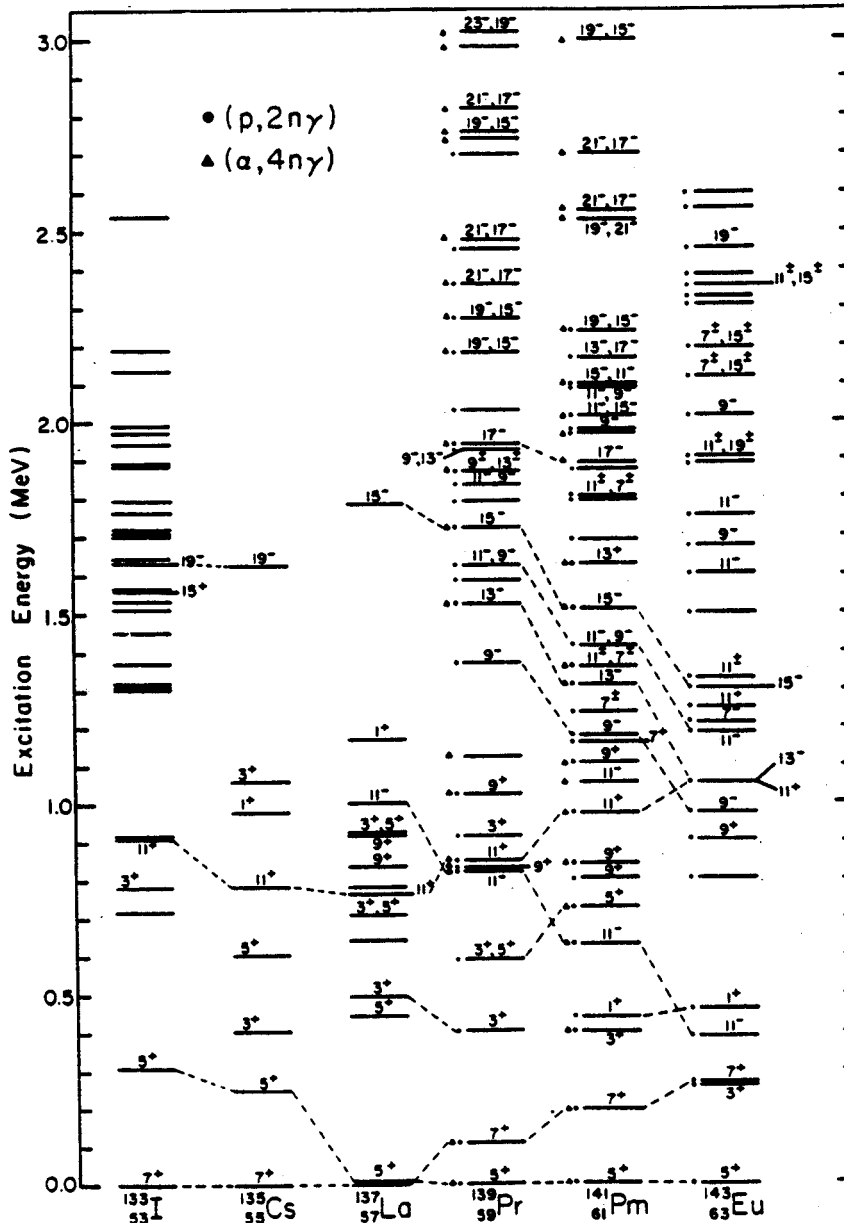


Fig. 3: Systematics of known states in odd-mass  $N = 80$  isotones. (The states above 3 MeV in  $^{139}\text{Pr}$  from the ( $\alpha$ , 4n $\gamma$ ) reaction are not shown.) Spins are shown as  $2J$ .

We performed a complete triaxial calculation by coupling the  $\pi h_{11/2}$ ,  $d_{5/2}$ , and  $g_{7/2}$  states to the  $2_1^+$ ,  $0_1^+$ ,  $2_2^+$ ,  $4_1^+$ , and  $3_1^-$  vibrational states in  $^{138}\text{Ce}$ . The results for the negative-parity states are shown in Fig. 4. The lowest excited states,  $2_1^+$  and  $4_1^+$ , of  $^{138}\text{Ce}$  were used to deduce the deformation parameter  $\beta$  and asymmetry parameter  $\gamma$ . Since the triaxial model cannot distinguish between prolate and oblate shapes in even-even nuclei, we calculated both. Oblate deformation leads to much better agreement with the experimental data, both in

terms of energy separations and ordering of the levels. Also, prolate deformation predicts an unobserved low-lying  $7/2^-$  state.

The calculated energies for  $(\pi_{11/2} \times 2_2^+)$  states are somewhat higher than their experimental counterparts by about 700 keV. Because of the spin uncertainties, complete correlations for these states are not possible. Similarly, the  $(\pi_{11/2} \times 4_1^+)$  states are calculated to lie near 3022 keV, much higher than the experimental values. For example, the  $17/2^-$  state is observed at 1941.6 keV, as

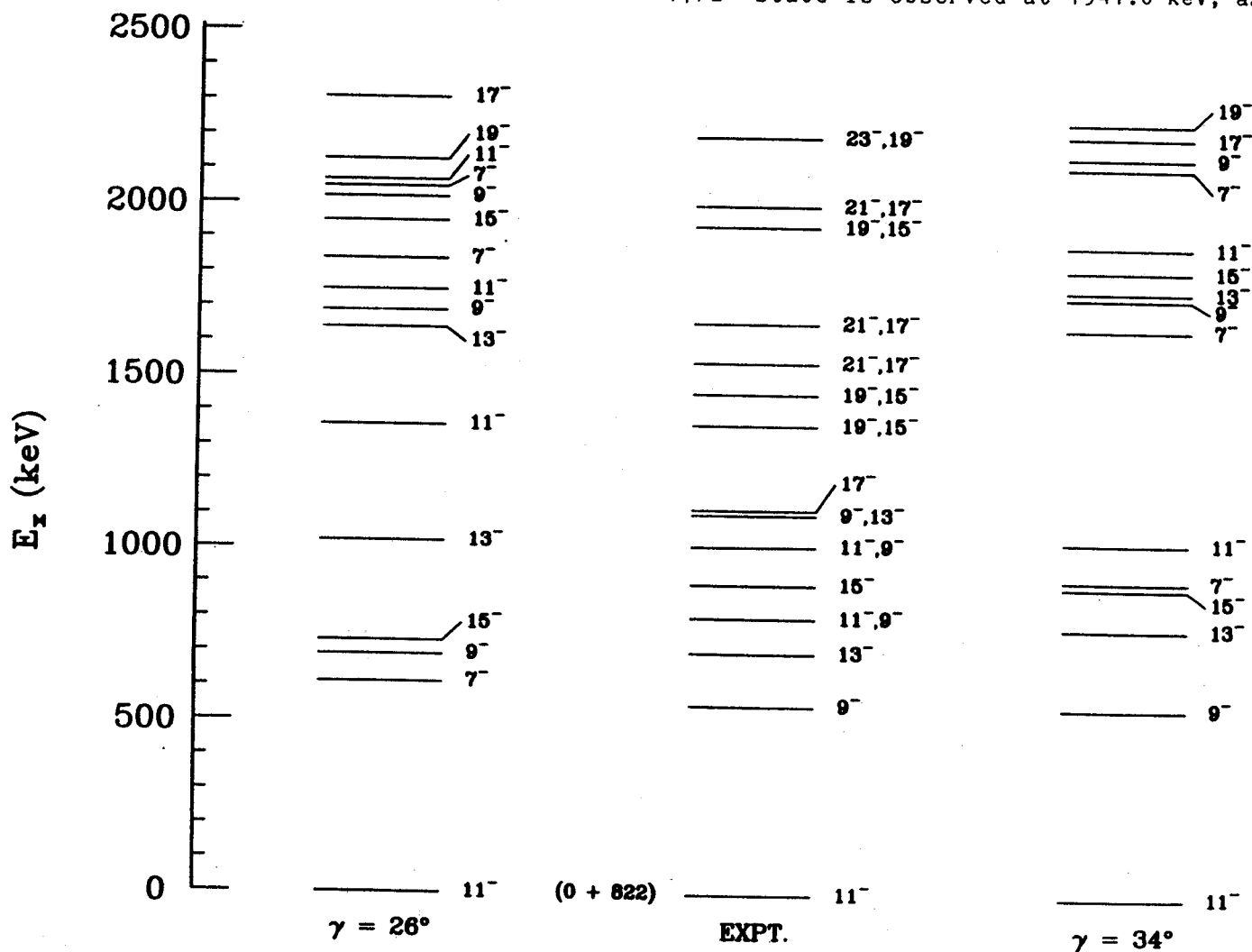


Fig. 4: Energies of negative-parity triaxial core-coupled states (for  $\beta = 0.153$ ,  $\lambda_f = 1.0$ , and  $\Delta = 0.97$ ) compared with our experimental results. The states on the left are for a prolate deformation, on the right for an oblate deformation. Spins are given as  $2J$ .

compared with a calculated value of 3022 keV. (Note that its  $\gamma$ -decay pattern goes largely through the  $(\pi h_{11/2} \times 2_1^+)$  states.) The odd-proton apparently softens the core, lowering the  $4_1^+$  state from its position in  $^{138}\text{Ce}$ .

### Positive-Parity Collective States

As expected, the triaxial model delivers poorer results for these states because of the plethora of possible structures and consequent ease of configuration mixing. The positive-parity states can be generated by coupling the

$\pi d_{5/2}$  and  $\pi g_{7/2}^{-1}$  states to the  $^{138}\text{Ce}$  core. The results are shown in Fig. 5. The  $(\pi d_{5/2} \times 2_1^+)$  states should lie near 790 keV. The  $\pi d_{3/2}$  state at 405 keV behaves experimentally more like the state in  $^{141}\text{Pm}$  (less fractionated) than the state in  $^{143}\text{Eu}$ . However, our calculations indicate this to be a  $5/2^+$  core-coupled state. The first  $9/2^+$  state is predicted to lie at 780 keV, in decent agreement with the observed state at 828 keV. The  $(\pi g_{7/2}^{-1} \times 2_1^+)$  coupling leads to observable  $5/2^+$ ,  $11/2^+$ ,  $3/2^+$ , and  $9/2^+$  states near 904 keV, all of which should deexcite

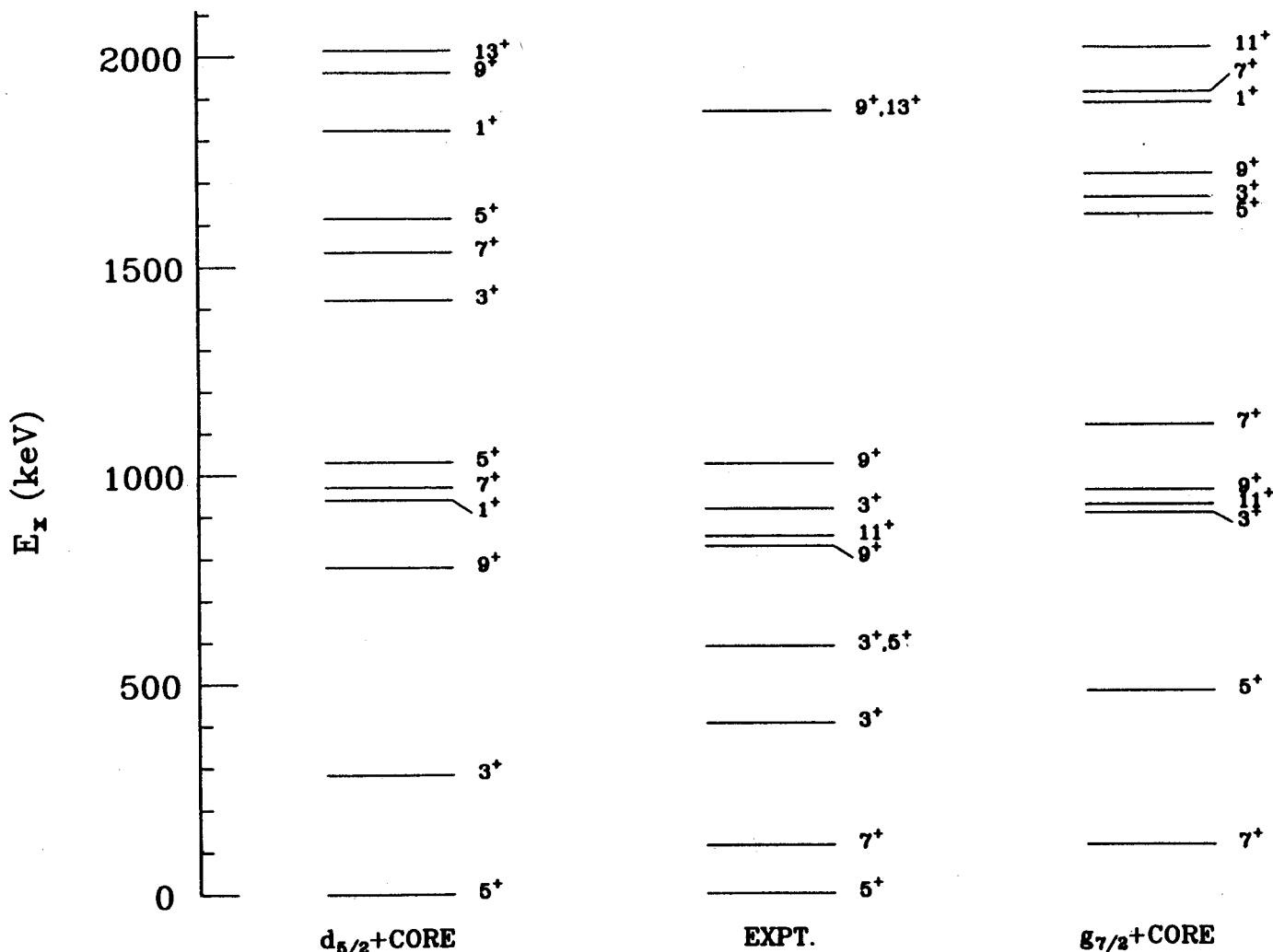


Fig. 5: Energies of positive-parity triaxial core-coupled states (same parameters as for Fig. 4) compared with our experimental results. Only  $\pi d_{5/2}$  and  $\pi g_{7/2}^{-1}$  states coupled to an oblate ( $\gamma = 34^\circ$ ) are shown. Spins are given in 2J.



predominantly through the 113.9-keV state, again in good agreement with the observed states at 590, 852, 917, and 1024. Little can be said about the remaining states because of the uncertainties in their assignments.

In summary, the triaxial model does reasonably well in describing the low-lying structures in these  $N = 80$  isotones. It predicts an oblate shape for these nuclei. However, the results for higher-lying states, especially the negative-parity states, are less satisfactory. It appears that separate core-shape parameters would be necessary to obtain adequate fits. Actually, our IBFA calculations do a much better job for the  $N = 80$  isotones, in general.

---

#### References

1. J. Meyer-ter-Vehn, Nucl. Phys. A249, 111 (1975).
2. F. Iachello and O. Scholten, Phys. Rev. Lett. 43, 679 (1979).
3. W.-T. Chou, Wm. C. McHarris, and Olaf Scholten, MSUCL-611, accepted for publication in Phys. Rev. C; also, see contribution on pge. 123 in this Annual Report.
4. R.W. Gales, R.A. Warner, and Wm.C. McHarris, Phys. Rev. C 6, 587 (1972).

S. Gil,<sup>a</sup> A. Garcia,<sup>a</sup> J. Gundlach,<sup>a</sup> D. Mikolas, T. Murakami, W. Olivier, and W.F. Rogers<sup>a</sup>

An exploratory run was performed in order to study the feasibility of using the reaction  $^3\text{He}(^{36}\text{Ar}, ^{37}\text{Ca})2n$  for producing  $^{37}\text{Ca}$ . Our objective was to determine the B(GT) distribution for the  $^{37}\text{Ca}$   $\beta^+$  decay by the measurement of the  $^{37}\text{K}$  delayed proton spectrum. This information is relevant in the determination of the solar neutrino capture cross section of  $^{37}\text{Cl}$ , which is important in light of the current solar neutrino problem.<sup>1,2</sup> The currently accepted cross section value is partially based on  $^{37}\text{Ca}$  delayed proton spectrum measurements by Sextro et al.<sup>3</sup> which were analyzed assuming that all  $^{37}\text{K}$  decays proceed to the  $^{36}\text{Ar}$  ground state. Adelberger and Haxton<sup>4</sup> have pointed out that neglecting decays to the first excited state of  $^{36}\text{Ar}$  at 1.97 MeV yields a B(GT) distribution that is too weak and shifted to lower excitation energies.<sup>5</sup> This effect produces a  $^{37}\text{Cl}$  neutrino capture cross section that is too low by roughly 4%. Our goal was to measure the B(GT) spectrum more accurately by taking account of proton decays to the  $^{36}\text{Ar}$  first excited state.

In this first experiment we have studied the feasibility of using the reaction  $^3\text{He}(^{36}\text{Ar}, ^{37}\text{Ca})2n$  at  $E_{\text{lab}} = 11.4$  MeV/A for producing  $^{37}\text{Ca}$  and separating this isotope using the Recoil Product Mass Separator (RPMS) facility at MSU.<sup>6</sup> This reaction is the kinematically reversed reaction used by Sextro et al. at about the same energy in the center of mass system.

Our experimental set up consisted of 15 cm long target gas cell filled with  $^3\text{He}$ . By changing the pressure of the gas, thicknesses between 2.5 and 3.5 mg/cm<sup>2</sup> of  $^3\text{He}$  were obtained. The gas was contained by 2 mg/cm<sup>2</sup> Havar window foils. The detector arrangement consisted of a three element telescope for particle

identification located in vacuum at the focal plane of the RPMS. Outside vacuum, several NaI detectors were positioned together with an intrinsic Ge detector just behind the chamber that contained the telescope. These gamma detectors were used for obtaining a further identification of the radioactive recoil products by their delayed gamma emissions.

The RPMS was calibrated by transporting the incident beam, which passed through the gas cell through the RPMS. Its focussed image was viewed on scintillators located alternately after the Wien filter and at the focal plane. Four individual charge states (+15, +16, +17, and +18) were clearly identified. The velocity region between 83% and 94% of the transported beam velocity was studied in detail, which broadly encompassed the  $^{37}\text{Ca}$  recoil products.

The particle spectrum was strongly dominated by inelastically scattered Ar particles and a few other ion species occurring close to zero degrees. The second most abundant element present was K. These two species dominated our spectra in all the various velocity windows which were investigated, as well as for all settings of the deflecting magnet. The high counting rate of these particles ( $\approx 3-5$  kHz) prevented us from increasing the beam current ( $\leq 10$  pA). We found no indication of  $^{37}\text{Ca}$  at the focal plane, presumably due to its very low production cross section, and to the restrictive circumstances in which we were forced to run.

Further analysis of the delayed  $\gamma$ -rays revealed no significant trace of radioactive products associated with the reaction  $^{36}\text{Ar} + ^3\text{He}$ . The activity observed by the Ge detector persisted for more than 20 minutes after the beam was shut off, and was most likely due to heavy neutron activation in the room.

These spectra did not change appreciably when we changed the gas inside the target cell ( $^4\text{He}$  and  $^{14}\text{N}$ ); from previous spectra taken with  $^3\text{He}$ , nor did they change when the target cell was emptied. We found virtually no counts in our detectors when the windows of the cell were removed, indicating no appreciable slit or beamline scattering of beam particles. Finally by introducing a pure Ni foil in place of a window we reproduced a spectrum similar to the original one, indicating that the window foils were indeed responsible for the vast majority of counts arriving at the focal plane. We also noted that the production yield of the windows did not seem to depend on window materials. The reaction mechanism which was more likely responsible for our observations is some type of quasi-elastic scattering which at near zero degrees produces beam-like particles with Z close to or equal to that of the beam, and with velocities that broadly span the region encompassing the fusion products of interest. Therefore the present reaction mechanism for producing  $^{37}\text{Ca}$  does not appear to be feasible when using a target gas cell with window. We next intend to study the possibility of using projectile fragmentation at high energies as a mean of producing  $^{37}\text{Ca}$ .

---

a. University of Washington, Seattle, Washington.

#### References

1. J.N. Bahcall, W.F. Huebner, S.H. Lubow, P.D. Parker, and R.K. Ulrich, Rev. Mod. Phys. 54, 767 (1982).
2. J.N. Bahcall, Rev. Mod. Phys. 50, 881 (1978).
3. R.G. Sextro, R.A. Gough, and J. Cerny, Nucl. Phys. A234, 130 (1974).
4. E.G. Adelberger and W.C. Haxon, Phys. Rev. C 36, 879 (1987).
5. J. Rapaport et al., Phys. Rev. Lett. 47, 1518 (1981).
6. J.A. Nolen Jr., L.H. Harwood, M.S. Curtin, E. Ormand and S. Briker, "Instrumentation for Heavy Ion Nuclear Research", Proc. of the Int. Conf. on Inst. for Heavy Ion Nuclear Research, ORNL, Tennessee, Oct. 22-25, (Harwood Academic Publishers, 1984).

W.-T. Chou, W. Olivier, Wm.C. McHarris, and O. Scholten<sup>a</sup>

In 1984 Kreiner et al. reported that a doubly-decoupled band, a  $\Delta I=2$  rotational band, has been observed in odd-odd  $^{186}\text{Ir}$ ,<sup>1,2</sup> which was possibly the first case of such a coupling scheme. Afterward they performed a series of experiments to look for this doubly-decoupled band in nearby odd-odd nuclei, and it has been observed in other Ir isotopes,<sup>3</sup> as well as in Re<sup>4,5</sup> and Ta.<sup>6</sup>

It was pointed out<sup>7</sup> that a system involving the  $1/2^- [541]$  (originating from the  $h_{9/2}$  spherical state) proton orbital and a low- $\Omega$  neutron orbital would in fact provide a natural explanation for this band. It is also believed that the state of lowest energy is not the state of minimum angular momentum, and the unfavored (positive signature) states are shifted above the corresponding favored ones. The lowest state of this band is  $5^+$  in the Ir isotopes, while it is believed to be  $3^+$  in the Re isotopes, although the  $5^+ \rightarrow 3^+$  transition has not been observed experimentally because its energy is too low.

We have performed IBFFA calculations for odd-odd Re nuclei near the region where such doubly-decoupled bands are found and have tried to look for this band in our calculations. The IBFFA calculations do predict the existence of this doubly-decoupled band in all three odd-odd Re nuclei we calculated, and they indicate that it is a coupling of the  $1/2^- [541]$  proton state with a  $K^\pi=1/2^-$  neutron state. However, since the excitation energies of this band are rather high in  $^{182,184}\text{Re}$ , they would not be expected to be observed in experiments. In fact, this band has been seen experimentally<sup>6</sup> only in  $^{180}\text{Re}$ . Figure 1 shows it compared with the predictions from our IBFFA calculations. The IBFFA calculation predicts the  $5^+ \rightarrow 3^+$  transition to be 45.7 keV. A  $\gamma$ -ray in this energy range is

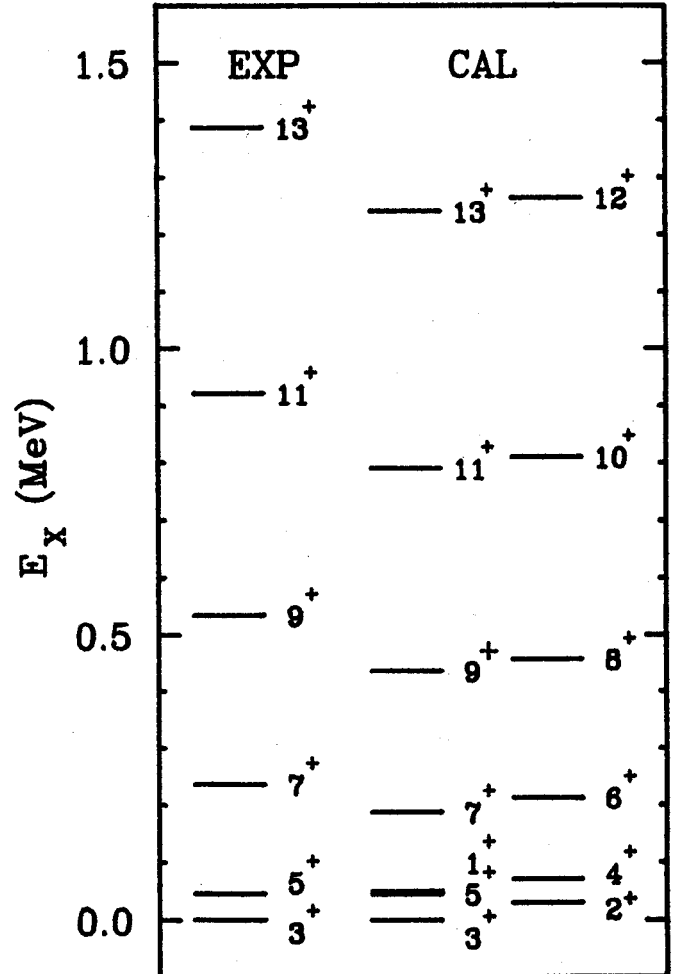


Fig. 1: Calculated vs. experimental results for the doubly-decoupled band in  $^{180}\text{Re}$ . The  $5^+ \rightarrow 3^+$  transition is too low in energy to be seen experimentally, so we used the calculated value (45.7 keV) for purpose of comparison.

highly converted and easily masked, which could explain why it was not observed experimentally. The spacings of our calculation are too small because of problems in fitting a  $K=1/2$  band<sup>8</sup> in the odd-mass nuclei (a problem inherent in all calculations). However, the important points we would like to address here are: 1) The calculation does predict  $3^+$  as the state of lowest energy, and 2) the coupling scheme is exactly the same as that proposed by Emery et

al.<sup>7</sup> Also, note that the unfavored states are shifted about 20 keV higher than the corresponding favored ones.

We were motivated by this satisfactory agreement and decided to extend IBFFA calculation to lighter odd-odd Re nuclei, where doubly-decoupled bands have also been found from our own experiments.<sup>9</sup> Fig. 2 shows results of our calculation for <sup>176,178</sup>Re compared with experimental data. Again, though it is our very first result, the IBFFA calculation was able to reproduce the feature of these bands. It is worth while mentioning that there is no experimental information about states in <sup>175</sup>Re, the proton of which couples with <sup>177</sup>Os to form <sup>176</sup>Re. The parameters we use in our calculations are chosen from systematics. This makes the agreement even more surprising, since until now it has not been thought possible to use systematics for odd-odd nuclei.

a. KVI, Groningen.

#### References

1. A. J. Kreiner, D. E. Di Gregorio, A. J. Fendrik, J. Davidson, and M. Davidson, Phys. Rev. C 29, 1572 (1984).
2. A. J. Kreiner, D. E. Di Gregorio, A. J. Fendrik, J. Davidson, and M. Davidson, Nucl. Phys. A432, 451 (1985).
3. P. Thieberger and E. K. Warburton, Phys. Rev. C 34, 1150 (1986).
4. J. Davidson, M. Davidson, M. Debray, G. Falcone, D. Hojman, A. J. Kreiner, I. Mayans, C. Pomar, and D. Santos, Z. Phys. A 324, 363 (1986).
5. A. J. Kreiner, J. Davidson, M. Davidson, D. Abriola, C. Pomar, and P. Thieberger, Phys. Rev. C 36, 2309 (1987).
6. A. J. Kreiner and D. Hojman, Phys. Rev. C 36, 2173 (1987).
7. G. T. Emery, R. Hochel, P. J. Daly, and K. J. Hofstetter, Nucl. Phys. A211, 189 (1973).
8. W.-T. Chou, Wm. C. McHarris, and O. Scholten, MSUNSCL-611 (accepted for publication by Phys. Rev. C).
9. R. Aryaeinejad, W.-T. Chou, W. A. Olivier, and Wm. C. McHarris, MSU Cyclotron Laboratory Annual report for 1987, pg. 104 and pg. 106.

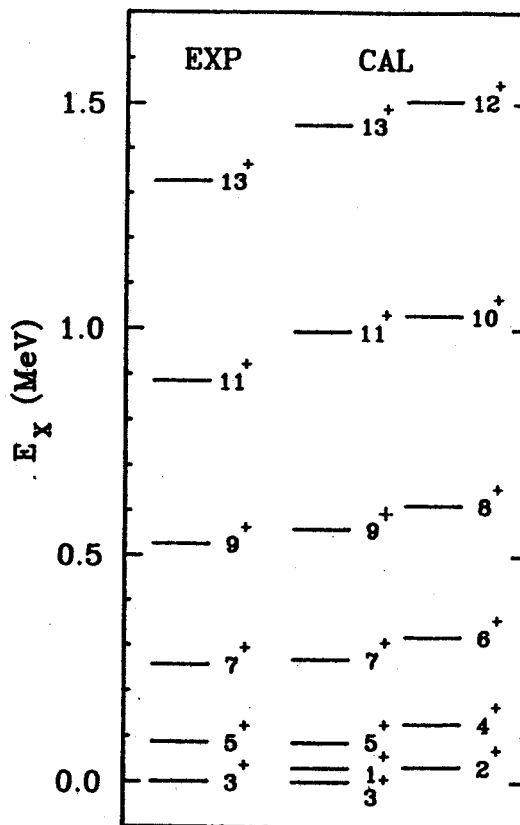
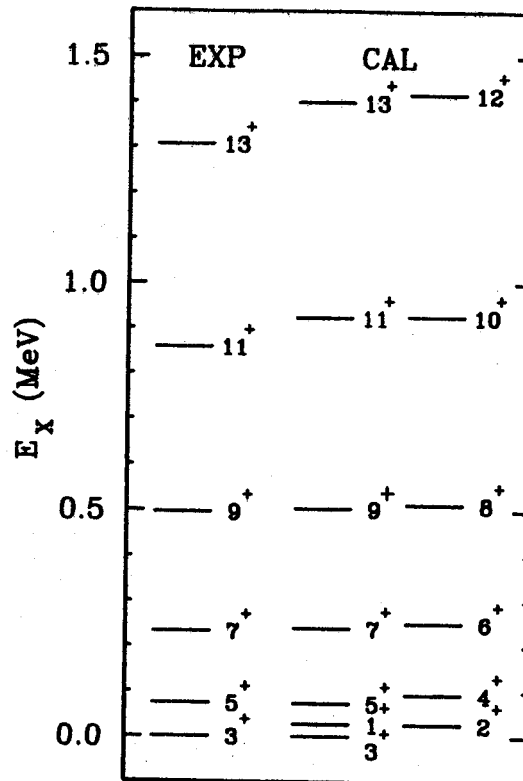


Fig. 2: Doubly decoupled bands of <sup>176,178</sup>Re. (a) <sup>178</sup>Re. (b) <sup>176</sup>Re. The calculated 5<sup>+</sup>→3<sup>+</sup> transition energy is used as in Fig. 1.

W.-T. Chou, Wm.C. McHarris, and O. Scholten<sup>a</sup>

Our studies for extending the IBA model to odd-odd nuclei have continued. The present article is the continuation of an article in the NSCL Annual Report for 1986.<sup>1</sup> Since the complete work has been submitted for publication,<sup>2</sup> we give only the results of our final calculations for odd-odd <sup>180-184</sup>Re nuclei, and draw some conclusions.

The results of in-beam studies of <sup>180</sup>Re<sup>3,4</sup> were not published until 1985, and assignments of the six rotational bands are considerably less certain for this nucleus than for <sup>182,184</sup>Re. In fact, our calculations are incompatible with the first tentative assignments made for some of the bands on the basis of M1/E2 mixing ratios.<sup>3</sup> Kreiner et al. recently reported their studies<sup>5</sup> of the same nucleus. Although there are still some uncertain assignments and unknown band-head energies, we are able to make comparisons with most of the Y-ray transition energies. Table 1 lists those transitions, along with our calculated energies. The comparisons for the intraband transitions in the first three bands are straightforward, while some questions arise for the last band,  $K^\pi=8^-$ . It was assigned as the coupling of  $\pi 9/2^- [514+]$  with  $\nu 7/2^+ [633+]$ , and it is strongly admixed with a  $K^\pi=9^-$  band, which is the coupling of  $\pi 9/2^- [514+]$  with  $\nu 9/2^+ [624+]$ . Our calculation confirms that the band is strongly admixed; however, it indicates the lowest state of the band to be  $9^-$  instead of  $8^-$ . What is observed in the isotones of <sup>180</sup>Re, <sup>181</sup>Os and <sup>179</sup>W, supports our calculations: A band is assigned as a mixed  $i_{13/2}$  band in <sup>181</sup>Os, with a  $9/2^+$  band-head; a  $9/2^+ [624+]$  band lies at 309 keV in <sup>179</sup>W; and  $7/2^+ [633+]$  at 477 keV. Thus, if we take into account the possibility of misassignment and compare the experimental

$9^- \rightarrow 8^-$  transition with the  $10^- \rightarrow 9^-$  transition in our calculations, etc., we see much better agreement. However more experimental evidence is needed to make any final judgement.

Table 1. Comparisons of experimentally observed Y-ray transitions with those predicted by calculation.

$K^\pi$	Transition	Exp(keV)	Cal(keV)
$8^+$	$9^+ \rightarrow 8^+$	228.7	210.9
	$10^+ \rightarrow 9^+$	246.0	236.5
	$11^+ \rightarrow 10^+$	261.4	260.2
	$12^+ \rightarrow 11^+$	275.4	277.0
$7^+$	$8^+ \rightarrow 7^+$	149.5	149.2
	$9^+ \rightarrow 8^+$	182.1	180.4
	$10^+ \rightarrow 9^+$	220.5	200.0
$5^+$	$7^+ \rightarrow 5^+$	191.1	142.5
	$9^+ \rightarrow 7^+$	297.8	248.0
	$11^+ \rightarrow 9^+$	386.4	354.2
	$13^+ \rightarrow 11^+$	465.6	451.1
	$15^+ \rightarrow 13^+$	514.6	560.1
$8^-$	$9^- \rightarrow 8^-$	134.3	---
	$10^- \rightarrow 9^-$	176.4	139.1
	$11^- \rightarrow 10^-$	210.1	185.5
	$12^- \rightarrow 11^-$	237.2	208.7
	$13^- \rightarrow 12^-$	261.0	231.2

A number of rotational bands have been observed in <sup>184</sup>Re, but only the ground-state  $3^-$  and an  $8^+$  band having its band-head at 188 keV have been given definite assignments.<sup>6</sup> We

show a comparison of our results with these data in Fig. 1. The spacings within the bands are reproduced quite well, but there are minor problems with the positions of the band-heads themselves. In particular, we calculate the  $2^-$  band-head to lie below the  $3^-$  band-head, whereas the reverse is observed. These states are the singlet and triplet couplings of the  $\pi 5/2^+[402^+]$  and the  $\nu 1/2^-[510^+]$  Nilsson states, and according to the Gallagher-Moszkowski coupling rules, the triplet should lie lower in energy than the singlet. However, there is considerable mixing of the  $1/2^-$  neutron states, especially  $1/2^-[521^+]$  and  $1/2^-[501^+]$ , in the odd-mass Os isotope calculations, so the question of triplet versus singlet couplings becomes a bit obscure.

The IBFFA model is able to give an accurate description of states in the odd-odd Re nuclei, as can be seen from the comparisons with experimental data. These odd-odd nuclei constitute a very stringent test of the model, because odd-odd nuclei do not provide the same sort of smoothly varying systematics as do other types of nuclei. Also, errors tend to accumulate: Any difficulties in describing the even-even cores and, particularly, the odd-mass states are compounded in the odd-odd systems. However, if good fits for the even-cores and for the odd-mass states can be obtained, then good spacings in the odd-odd nuclei are likely. This can be seen in our calculations, where the poorest fits obtained for odd-mass states were for the  $1/2^-$  bands in the odd-mass Os isotopes.

$^{184}_{75}\text{Re}$

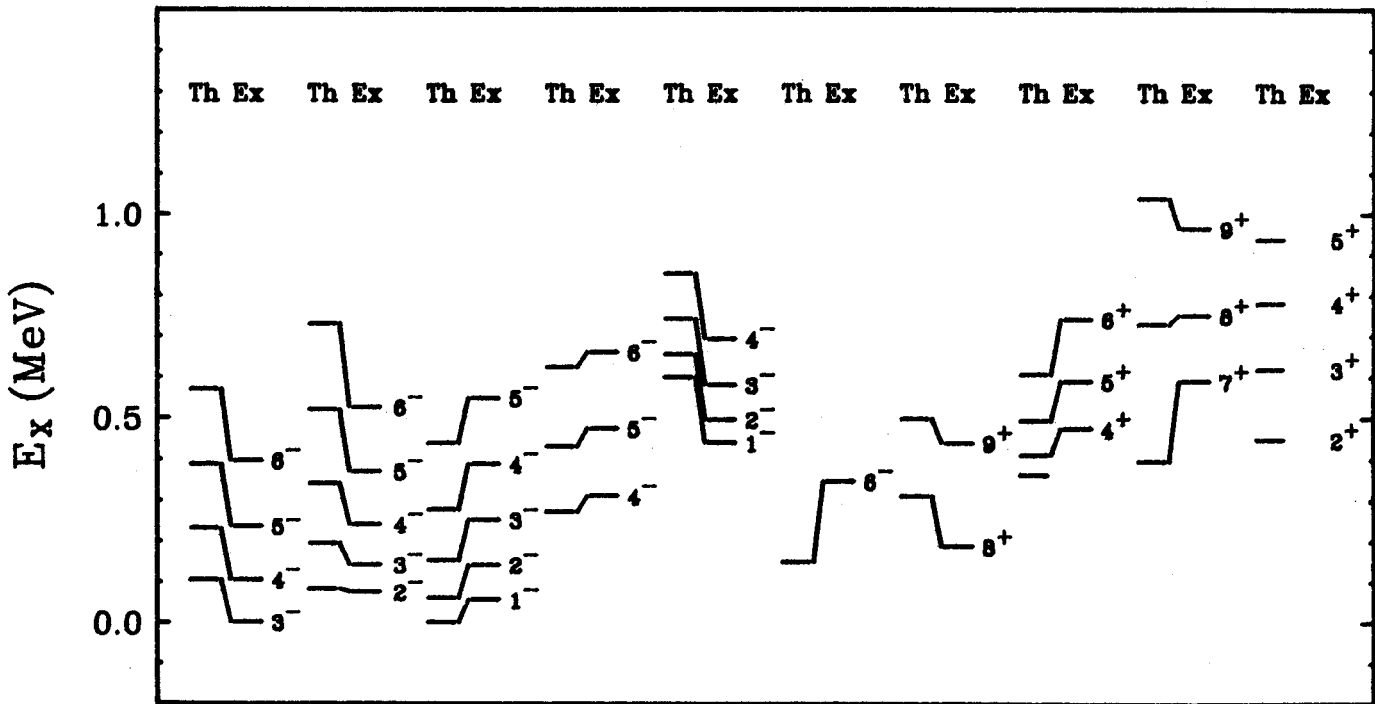


Fig. 1: The calculated excitation energy spectrum of  $^{184}\text{Re}$  compared with experimental data.

Correspondingly, relatively poor fits were obtained for odd-odd bands involving these  $1/2^-$  neutrons, such as inverting the triplet and singlet couplings. Also, in  $^{182}\text{Re}$  the  $4^-$  band, which involves a  $1/2^-$  proton, had the poorest fit. (Of course, adequate fits to  $J = 1/2$  bands are an inherent problem in any description, not just limited to an IBFA model.) In general, we obtained good fits for spacings within the bands but had some problems with the positions of the band-heads and with the triplet-singlet coupling spacings. This points to difficulties in  $V_{pn}$ , the proton-neutron residual interaction. (Again, this is recognized as a decades-old problem with calculations involving odd-odd nuclei.) A simple first-stage improvement would be to free  $V_q$  and especially  $V_s$ , allowing them to vary over a reasonable range. In addition, it should be remembered that in the present calculations we did not need to introduce an attenuation in the coriolis force.

---

a. KVI, Groningen

#### References

1. W.-T. Chou, Wm.C. McHarris, and O. Scholten, MSU Cyclotron Laboratory Annual Report for 1986, p. 99.
2. W.-T. Chou, Wm.C. McHarris, and O. Scholten, MSUCL-611 (accepted for publication by Phys. Rev. C).
3. R.M. Lieder, XXIII International Winter Meeting on Nuclear Physics, Bormio, Italy: Proceedings, p.276 (1985).
4. Ts. Venkova, R.M. Lieder, T. Morek, W. Gast, G. Hebbinghaus, A. Krämer-Flecken, J. Schäffler-Kräh, W. Urban, H. Kluge, K.H. Maier, A. Maj, and G. Sletten, KFA Jülich, Annual Report for 1985.
5. A.J. Kreiner, J. Davidson, M. Davidson, D. Abriola, C. Pomar, P. Thieberger, Phys. Rev. C 36, 2309 (1987).
6. M.J. Martin and P.H. Stelson, Nucl. Data Sheets 21, 1 (1977).